Science of the Total Environment 619–620 (2018) 1394–1408

Contents lists available at ScienceDirect

Science of the Total Environment

journal homepage: www.elsevier.com/locate/scitotenv

Modeling the hydrological impacts of land use/land cover changes in the Andassa watershed, Blue Nile Basin, Ethiopia

Temesgen Gashaw [a,c,*], Taffa Tulu [a], Mekuria Argaw [a], Abeyou W. Worqlul [b]

[a] Center for Environmental Science, College of Natural and Computational Sciences, Addis Ababa University, Ethiopia
[b] Blackland Research and Extension Center, Texas A&M Agrilife Research, TX, USA
[c] Department of Natural Resource Management, College of Agriculture and Environmental Science, Adigrat University, Ethiopia

HIGHLIGHTS

- There were expansions of cultivated land and built-up area, and withdrawing of forest, shrubland and grassland during the 1985–2015 periods, which are expected to continue in the 2030 and 2045 periods.
- The LULC changes, which had occurred during the period of 1985 to 2015, had increased the annual and wet season flow, surface runoff and water yield while the dry season flow, lateral flow, groundwater flow and ET were reduced.
- The 2030 and 2045 LULC states are expected to affect the hydrological components with the same direction.

GRAPHICAL ABSTRACT

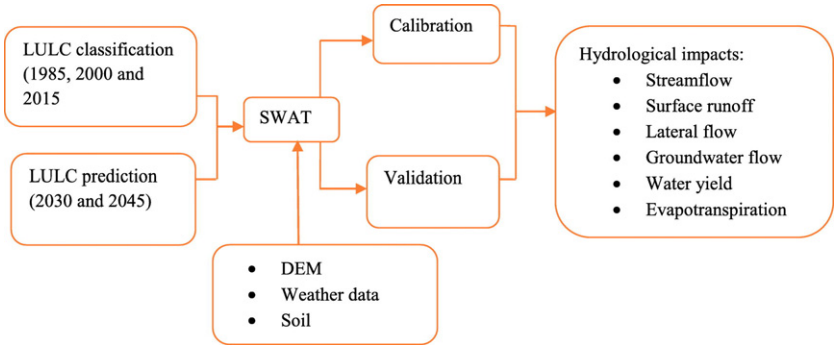

ARTICLE INFO

Article history:
Received 1 October 2017
Received in revised form 16 November 2017
Accepted 16 November 2017
Available online 24 November 2017

Keywords:
Land use/land cover
CA-Markov
Hydrology
Modeling
SWAT
PLSR

ABSTRACT

Understanding the hydrological response of a watershed to land use/land cover (LULC) changes is imperative for water resources management planning. The objective of this study was to analyze the hydrological impacts of LULC changes in the Andassa watershed for a period of 1985–2015 and to predict the LULC change impact on the hydrological status in year 2045. The hybrid land use classification technique for classifying Landsat images (1985, 2000 and 2015); Cellular-Automata Markov (CA-Markov) for prediction of the 2030 and 2045 LULC states; the Soil and Water Assessment Tool (SWAT) for hydrological modeling were employed in the analyses. In order to isolate the impacts of LULC changes, the LULC maps were used independently while keeping the other SWAT inputs constant. The contribution of each of the LULC classes was examined with the Partial Least Squares Regression (PLSR) model. The results showed that there was a continuous expansion of cultivated land and built-up area, and withdrawing of forest, shrubland and grassland during the 1985–2015 periods, which are expected to continue in the 2030 and 2045 periods. The LULC changes, which had occurred during the period of 1985 to 2015, had increased the annual flow (2.2%), wet seasonal flow (4.6%), surface runoff (9.3%) and water yield (2.4%). Conversely, the observed changes had reduced dry season flow (2.8%), lateral flow (5.7%), groundwater flow (7.8%) and ET (0.3%). The 2030 and 2045 LULC states are expected to further increase the annual and wet season flow, surface runoff and water yield, and reduce dry season flow, groundwater flow, lateral flow and ET. The change in hydrological components is a direct result of the significant transition from the vegetation to non-vegetation cover in the watershed. This suggests an urgent need to regulate the LULC in order to maintain the hydrological balance.

* Corresponding author at: Center for Environmental Science, College of Natural and Computational Sciences, Addis Ababa University, Ethiopia.
E-mail address: temesgen.gashaw@aau.edu.et (T. Gashaw).

https://doi.org/10.1016/j.scitotenv.2017.11.191
0048-9697/

1. Introduction

Land use/land cover (LULC) change has become a global concern (Woldeamlak, 2002) because of its diverse environmental impacts (Fu et al., 2000; Gete and Hurni, 2001; Woldeamlak, 2002; Lambin et al., 2003; Hurni et al., 2005). Globally, expansions of cropland and pasture land at the cost of forest, natural grassland and savannas were observed during the period of 1770–1990 and 1700–1990, respectively (Lambin et al., 2003). However, the direction of LULC change was not uniform across the world. In temperate region, forested areas are increasing by almost 3 x 10^6 ha/yr, while the tropical forests are decreasing by 12 x 10^6 ha/yr (MEA, 2005). LULC change is also one of the fundamental environmental problems in Ethiopia (Kebrom and Hedlund, 2000; Gete and Hurni, 2001; Gessesse and Kleman; 2007; Abate, 2011; Ebrahim and Mohamed, 2017). There was a rapid expansion of cultivated land at the expense of forest lands mostly in the highlands of the country (Gete and Hurni, 2001; Solomon et al., 2010; Rientjes et al., 2011; Gebremicael et al., 2013; Temesgen et al., 2014; Ebrahim and Mohamed, 2017). In the northern highlands of Ethiopia, there are few remnant forests, which are found in sacred and inaccessible places (Bongers et al., 2006), and cultivation is stretched to the steepest areas where access is naturally restricted (Gete and Hurni, 2001).

LULC changes are important driving forces of environmental changes across all spatial and temporal scales. LULC change contributes significantly to earth atmosphere interactions, forest fragmentations and biodiversity losses (Fu et al., 2000). It is also one of the factors contributing to climate change (Lambin et al., 2003). Climate change, in reverse, drives LULC change though its effect is felt after an extended period of time (Woldeamlak, 2002). Furthermore, LULC change is also responsible for altering the hydrological response of watersheds (Hurni et al., 2005; Girmay et al., 2009; Setegn et al., 2009; Sriwongsitanon and Taesombat, 2011; Gebremicael et al., 2013; Neupane and Kumar, 2015). Several studies have reported the impacts of LULC changes on streamflow (Rientjes et al., 2011; Getachew and Melesse, 2012; Gebremicael et al., 2013; Gwate et al., 2015; Kidane and Bogale, 2017). For example, the conversion of forest to agriculture between 1985 and 2011 periods in Angereb watershed, Ethiopia has increased the mean wet flow by 39% and decreased the dry average flow by 46% (Getachew and Melesse, 2012). The increased streamflow in Quaternary Catchment, South Africa during the 2004 and 2013 periods was also observed due to the expansion of cultivated land (92%) and the decrease of wooded land (35%) and grasslands (9.8%) (Gwate et al., 2015). The increase of wet season flow (peak flow) and reduction of dry season flow (baseflow) at El Diem station of Blue Nile Basin during 1970–2010 were also attributed to the conversion of vegetation covers into agriculture and grasslands over large areas of the basin (Gebremicael et al., 2013). Changes in farmland, forest and urban areas in upper Du watershed, China between 1978 and 2007 were also affected streamflow (Yan et al., 2013). Other studies in Chemoga watershed (Woldeamlak and Sterk, 2005), Upper Gilgel Abbay catchment (Rientjes et al., 2011) and Gedeb catchment (Koch et al., 2012; Tekleab et al., 2013), have also reported considerable effects of LULC changes on streamflow.

It is also evident that surface runoff is lower and groundwater flow is higher in vegetative lands due to the greater infiltration of rainfall into the shallow and deep aquifer. In bare lands, where vegetation is absent, surface runoff is higher and groundwater flow is lower (Woldeamlak and Sterk, 2005; Gyamfi et al., 2016). An example of this phenomenon is the study in Comet catchment of Australia where the clearing of forest vegetation from 83% to 38% increased the runoff by approximately 40% (Siriwardena et al., 2006). Similarly, increasing of surface runoff and reduction of groundwater flows were also reported in Olifants basin, South Africa between 2000 and 2013 due to the expansion of cultivated lands and urban areas at the expense of rangelands (Gyamfi et al., 2016). Other studies have also reported the increase of surface runoff due to the expansion of cultivated lands and reduction of vegetative covers (Nie et al. (2011) in the upper San Pedro watershed, Mexico; Karamage et al. (2017) in Rwanda; Tekalegn et al. (2017) in Lake Tana catchment and Beles watershed, Ethiopia).

The study area (Andassa watershed) is a part of the northwestern Ethiopian highlands. It is known to be one of the most productive areas in the country and it is the head stream of the Blue Nile River. However, the watershed suffers from human-induced resource degradation mainly due to agricultural expansion and generally unregulated LULC change. The impacts of such changes on the hydrology are poorly understood. Hence, thorough analyses and understanding of impacts of LULC changes on the hydrology is critically important for planning the management of water resources in particular and the entire watershed in general. Because of its strategic importance to maintain a continuous of flow of water to the Blue Nile River; one of the major tributaries of the transnational Nile River, the findings of this study from the Andasa watershed will be of value not only for the management of the land resources in the watershed but also for the management of soil erosion and sedimentation as well as maintaining a constant water flow to the larger Nile Basin within and beyond the national boundary. The main aim of the study is, therefore, capturing the hydrological impacts of the past and future LULC changes in the watershed and translating the results into a management decision in order to overcome the negative consequences of such changes on the hydrological balance of the Andassa watershed as well as the broader upper Blue Nile Basin.

2. Materials and methods

2.1. Description of the study watershed

The Andassa watershed is part of the headstream areas of the Blue Nile River and it is located at about 560 km northwest of Addis Ababa and in a close proximity to Bahir Dar, which is the regional capital. Geographically, it is found between 11°08′–11°32′ N and 37°16′–37°32′ E (Fig. 1). The watershed with a surface area of 58,760 ha is situated in three administrative districts or '*Woredas*', vis, Bahir Dar Zuria, Mecha and Yilmana Densa. The topography of the Andassa watershed is hilly with elevation ranging from 1701 m to 3216 m a.s.l. Its agro-climate is remarkably dominated by sub-tropical climate (85.2%) with a small segment of temperate climate (14.8%). According to the data obtained from the GIS department of Ethiopian Ministry of Water and Energy (EMWE), the watershed geology is characterized by Alluvium, Ashangi basalts, basalts related to volcanic center and Termaber basalts. Andassa River, which traverses the watershed, is the major river within the watershed and is also a tributary to the Blue Nile River. Agriculture is the predominant economic activity in the watershed and the main source of livelihood.

2.2. Land use/land cover change assessment

Assessments of LULC were undertaken using three Landsat images; Landsat-5 TM 1985, Landsat-7 ETM^+ 2000 and Landsat-8 OLI_TIRS 2015. The images with 30 m resolution and cloud cover of 0 were collected from U.S Geological Survey (USGS) Center for Earth Resources Observation and Science (EROS) (https://earthexplorer.usgs.gov/).The hybrid classification technique (Teferi et al., 2010; Solomon et al., 2014), which involves unsupervised classification followed by supervised classification technique, was employed in classifying the images. Unsupervised classifications were carried out using Iterative Self-Organizing Data Analysis (ISODATA) clustering algorithm (Boakye et al., 2008; Teferi et al., 2010) while supervised classifications were undertaken with Maximum Likelihood Classification (MLC) algorithm (Solomon et al., 2014; Temesgen et al., 2014) by collecting 450 ground truth samples from the five LULC classes (75 GPS points in each LULC). The LULC classes were cultivated land, forest, shrubland, grassland and built-up area. In classifying the 1985 and 2000 images, reference data from Google Earth images of the corresponding time periods were

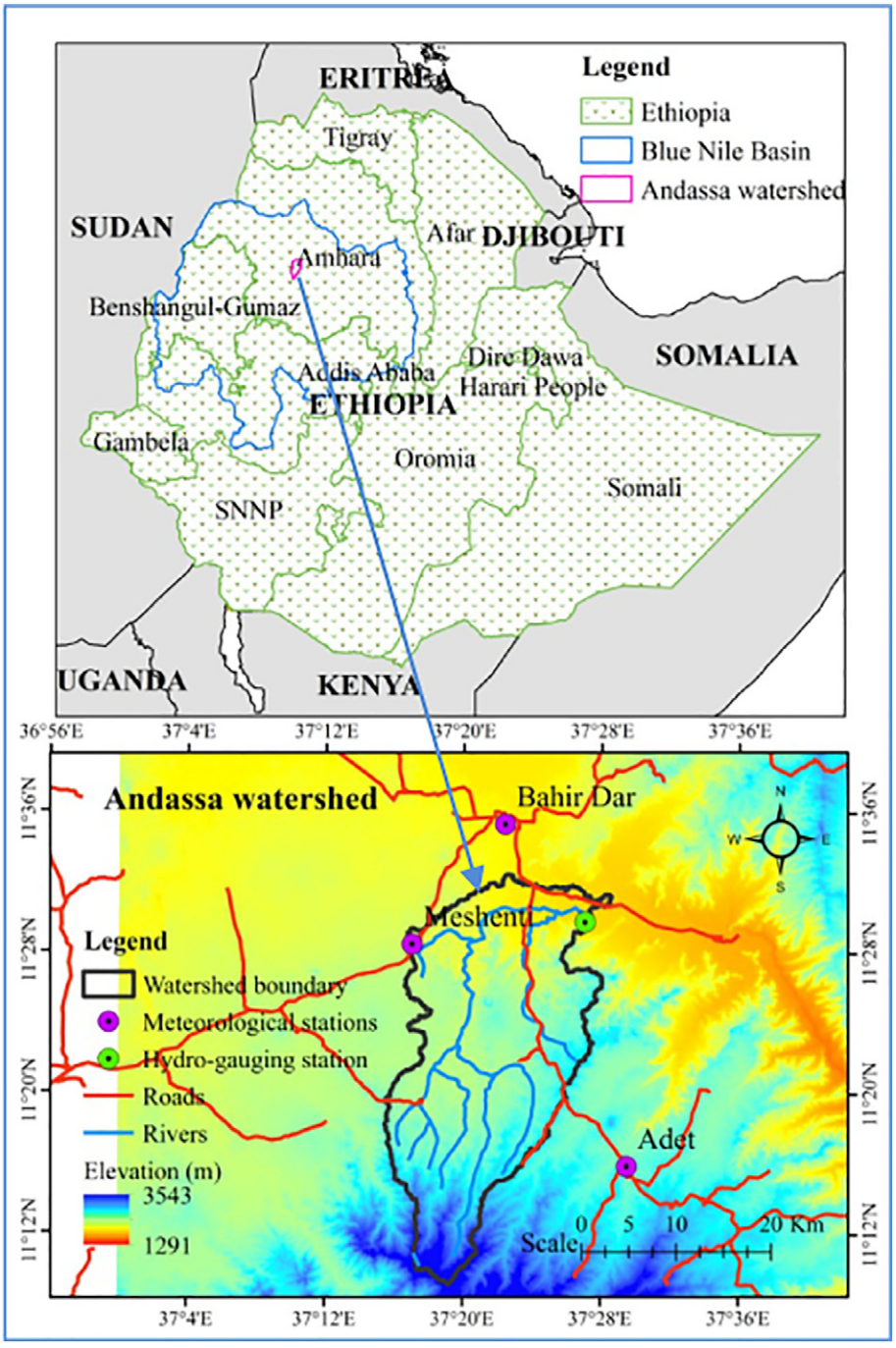

Fig. 1. Location of the study area, and meteorological and hydro-gauging stations in the Andassa watershed.

collected. Geo-linking techniques and in-depth focus group discussions with local elders were also undertaken. Accuracy assessment was employed with reference to the corresponding Google Earth images (i.e. 05 February, 1985; 21 February, 2000 and 28 February, 2015, respectively) to illustrate the representativeness of the classified images on the ground. ERDAS 2014 was used for image classifications purpose and ArcGIS 10.3 for mapping purposes.

2.3. Land use/land cover prediction

Cellular Automata-Markov (CA-Markov) model was used to predict the 2030 and 2045 LULC status. CA-Markov available in IDRISI 17.0 is a robust model that predicts the trend and the spatial structure of different LULC categories (Arsanjani et al., 2011; Wang et al., 2012; Li et al., 2015) based on historical LULC image, transition probability matrix and suitability images as a group file (Clark Labs, 2012; Eastman, 2012). This model is also widely applied in many countries (Wang et al., 2012; Omar et al., 2014; Singh et al., 2015; Mosammam et al., 2016). CA-Markov projection relies on past trends; the model does not take into account changes in the land-use policies during the projection period. The study employed the 2015 classified map as basis LULC image, and the 2000 and 2015 maps for assembly transition probability matrix. CA-Markov considers factors and constraints for preparing a single suitability maps (Clark Labs, 2012; Eastman, 2012; Omar et al., 2014; Singh et al., 2015). Factors are criterions that indicate the relative suitability of areas under consideration while constraints are criterions

which limit the alternatives under consideration (Clark Labs, 2012; Eastman, 2012). The factors and constraints considered in this study were distance to river, distance to town, distance to road, proximate to developed area, suitable areas for conversion to each class, elevation and slope. River and road data were obtained from the GIS department of EMWE while data such as distance to town, proximate to developed area and suitable areas for conversion to each class were derived from the classified maps. Elevations and slopes were generated from 30 m resolution of ASTER Global Digital Elevation Model (ASTER GDEM), which was obtained from Aster Global Digital Elevation Map (http://gdex.cr.usgs.gov/gdex/). A set of relative weights for a group of factors were assigned through in-depth focus group discussions with agricultural development agents and local elders, and an acceptable consistency ratio were obtained (see Temesgen et al. (2017) for detail). The factors and constraint were integrated using a Multi-Criteria Evaluation (MCE) decision support system with Weighted Liner Combination (WLE) fuzzy membership function to produce a single suitability map for each class. The considered factors and constraint and the prepared suitability maps for each LULC class are found in the Appendix. The detail discussions about the procedures followed in the prediction of LULC states is available in Temesgen et al. (2017).

The model was validated by simulating the 2015 LULC state using the 1985 and 2000 classified images. Then, the agreements of the simulated and the classified 2015 LULC maps were compared using the "Relative Operating Characteristic (ROC)" (Pontius and Schneider, 2001) and Kappa indexes (Mosammam et al., 2016) such as Kappa for no information (*K*no), Kappa for location (*K*location), Kappa for stratum-level location (*K*locationStrata) and Kappa for standard (*K*standard) (Clark Labs, 2012; Omar et al., 2014; Mosammam et al., 2016).

2.4. Land use/land cover change analysis

Change analysis was carried out using the classified (1985, 2000 and 215) and the predicted LULC (2030 and 2045) states to demonstrate the pattern of LULC changes. To elucidate the extent of changes experienced between the subsequent periods (1985–2000, 2000–2015, 2015–2030

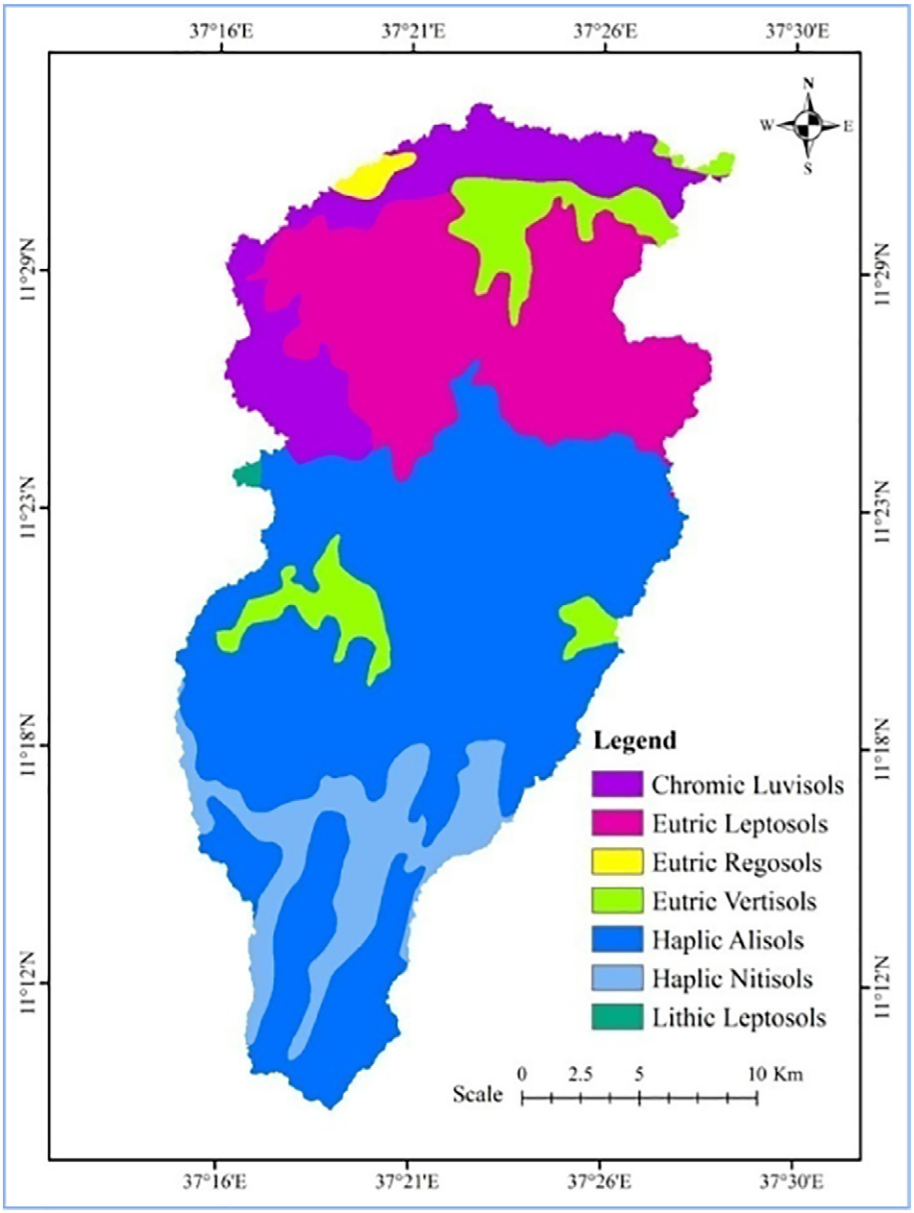

Fig. 2. Soil types of the Andassa watershed.

and 203–2045), percent of change (Ebrahim and Mohamed, 2017) and rate of change (Abate, 2011; Temesgen et al., 2014) were computed using Eqs. (1) and (2), respectively.

$$\text{Percent of change} = \left(\frac{X-Y}{Y}\right) \times 100 \quad (1)$$

$$\text{Rate of change (ha/yr)} = \left(\frac{X-Y}{Z}\right) \quad (2)$$

where X is area of LULC (ha) in time 2, Y is area of LULC (ha) in time 1, Z is Time interval between X and Y in years.

2.5. SWAT model inputs and analysis

2.5.1. SWAT model

The Soil and Water Assessment Tool (SWAT) is a physically based model developed in 1990s. It was designed to predict the impact of land management practices on water, sediment and agricultural chemical yields in large complex watersheds with varying conditions over long periods of time (Arnold et al., 1998; Neitsch et al., 2002; Setegn et al., 2008; Neitsch et al., 2011, Arnold et al., 2012b). The model predicts the impacts at the sub basin (sub watershed) or further at the Hydrologic Response Units (HRUs) (Githui et al., 2009; Tibebe and Bewket, 2011; Ghoraba, 2015). HRUs are portion areas within the sub-basin that are comprised of unique land cover, soil and slope combinations (Setegn et al., 2008; Arnold et al., 2011; Arnold et al., 2012b; Kushwaha and Jain, 2013). Categorizing sub-basins into HRUs increases accuracy and provides a much better physical description. The predicted values from each HRU are routed to obtain the total value for the watershed (Neitsch et al., 2002; Githui et al., 2009; Arnold et al., 2011). SWAT requires diverse information to setup and run the model. Specific information required for SWAT includes weather, hydrology, soil, topography and land use data (Neitsch et al., 2002; Githui et al., 2009; Yan et al., 2013). SWAT can model the physical process associated with water movement, sediment movement, crop growth, nutrient cycling etc. (Neitsch et al., 2002; Easton et al., 2010).

SWAT simulates the land phase of the hydrological cycle based on the water balance equation (Arnold et al., 1998) as shown in Eq. (3).

$$SW_t = SW_o + \sum_{i=1}^{t}(R_{day} - Q_{sur} - E_a - W_{seep} - Q_{gw}) \quad (3)$$

where SW_t is the final soil water content (mm); SW_o, R_{day}, Q_{sur}, E_a, W_{seep} and Q_{gw} are the initial soil water content, the amount of precipitation, the amount of surface runoff, the amount of evapo-transpiration, the amount of water entering the vadose zone from the soil profile and the amount of return flow on day i (mm), respectively; and t is the time (days).

Runoff in SWAT can be estimated either with the Soil Conservation Service (SCS) curve number (CN) method (USDA-SCS, 1972) or the Green and Ampt infiltration method (Green and Ampt, 1911). The SCS CN method was employed in this study. It is computationally efficient and the most popular method, which predicts runoff with a given rainfall event (Tibebe and Bewket, 2011; Ghoraba, 2015) mainly based on land use, soil properties and hydrologic conditions (Ghoraba, 2015). The SCS CN method computes runoff using Eq. (4) (Setegn et al., 2008; Tibebe and Bewket, 2011; Ghoraba, 2015).

$$Q_{sur} = \frac{(R_{day} - 0.2S)^2}{(R_{day} + 0.8S)} \quad (4)$$

where Q_{surf} is the daily surface runoff (mm), R_{day} is the rainfall depth for the day (mm), and S is the retention parameter (mm). The retention parameter (S) (Setegn et al., 2008; Tibebe and Bewket, 2011; Ghoraba, 2015) is given in Eq. (5).

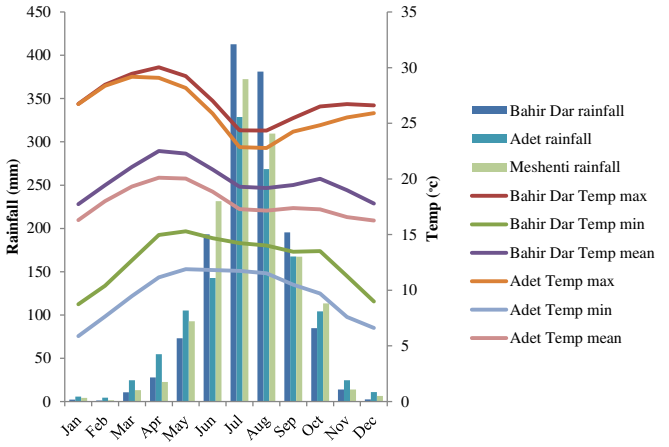

Fig. 3. Mean monthly rainfall and temperature (1990–2011) characteristics of the stations in the Andassa watershed.

$$S = 25.4\left(\frac{1000}{CN} - 10\right) \quad (5)$$

where S is drainable volume of soil water per unit area of saturated thickness (mm/day), CN is curve number

SWAT works in different GIS interfaces such as in AVSWAT (ArcView interface) (Tibebe and Bewket, 2011), ArcSWAT (ArcGIS interface) (Setegn et al., 2008; Getachew and Melesse, 2012; Kushwaha and Jain, 2013; Ghoraba, 2015; Huang and Lo, 2015; Begou et al., 2016) and QSWAT (Quantum GIS interface) (Dila et al., 2016). ArcSWAT2012 was employed in this study. The model has continuously expanded its capabilities throughout the years. The most significant improvement of the model since its release was made through the different stages of SWAT review. These were SWAT94.2, SWAT96.2, SWAT98.1, SWAT99.2, SWAT2000, SWAT2009 (Neitsch et al., 2011) and SWAT2012. The improvement of capabilities taken place in each stage of SWAT review is detailed in Neitsch et al. (2011). Further reading

Table 1
Flow parameters considered for calibration and validation of the SWAT model.

No.	Input parameter	Description
1	CN2.mgt	SCS runoff curve number
2	SURLAG.bsn	Surface runoff lag time
3	OV_N.hru	Manning's "n" value for overland flow
4	ALPHA_BF.gw	Baseflow alpha factor (days)
5	GW_DELAY.gw	Groundwater delay (days)
6	GWQMN.gw	Threshold depth of water in the shallow aquifer required for return flow to occur (mm)
7	GW_REVAP.gw	Groundwater "revap" coefficient
8	REVAPMN.gw	Threshold depth of water in the shallow aquifer for "revap" to occur (mm)
9	RCHRG_DP.gw	Deep aquifer percolation fraction
10	ESCO.hru	Soil evaporation compensation factor
11	EPCO.hru	Plant uptake compensation factor
12	CANMX.hru	Maximum canopy storage
13	SL_SUBBSN.hru	Average slope length
14	HRU_SLP.hru	Average slope steepness
15	CH_N2.rte	Manning's "n" value for the main channel
16	CH_K2.rte	Effective hydraulic conductivity in main channel alluvium
17	SOL_AWC.sol	Available water capacity of the soil layer
18	SOL_K.sol	Saturated hydraulic conductivity
19	SOL_Z.sol	Depth from soil surface to bottom of layer

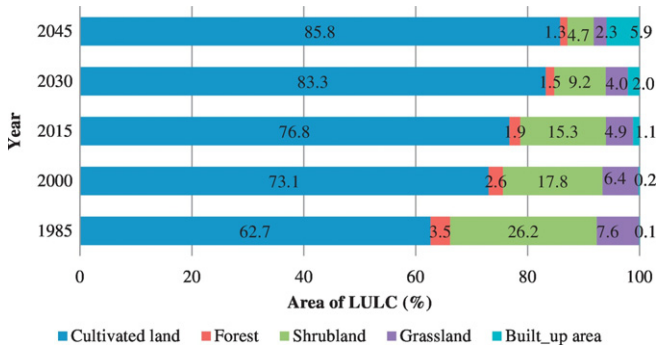

Fig. 4. Area of LULC (%) in the Andassa watershed through 1985 to 2045 periods.

material about SWAT model can be referred from Arnold et al. (1998) and the online resources at http://swat-model.tamu.edu/.

2.5.2. Data inputs

Spatial data such as DEM, LULC and soil, and temporal data such as climate and streamflow, which are required for SWAT as inputs, were secured as detailed below.

2.5.2.1. Digital elevation model (DEM). DEM were the first inputs of the SWAT model. The type of DEM used for the SWAT model in this study was ASTER GDEM. The ASTER GDEM was used for flow direction and flow accumulation calculation, drainage network generation, watershed delineation, sub basin definition and HRUs setup. The topographic parameters of the studied watershed such as terrain slope, channel slope or reach length were also derived from ASTER GDEM. Based on the topographic characteristics, the SWAT model had identified 13 sub basins in the studied watershed. The DEM and drainage networks of the studied watershed are shown in Fig. 1.

2.5.2.2. Land use/land cover. LULC maps were important component of the SWAT model. Therefore, the classified (1985, 2000 and 2015) and the predicted LULC (2030 and 2045) maps were used independently to uncover the hydrological impacts of LULC changes in the study watershed. The SWAT model requires a conversion of the LULC types into the four digits of the SWAT code. The SWAT codes given for cultivated land, forest, shrubland, grassland and built-up area were AGRC (Agricultural Land-Close-grown), FRST (Forest-Mixed), RNGB (Range-Brush), RNGE (Range-Grasses) and URBN (Residential), respectively. The detail descriptions of the five LULC types can be found in Temesgen et al. (2017).

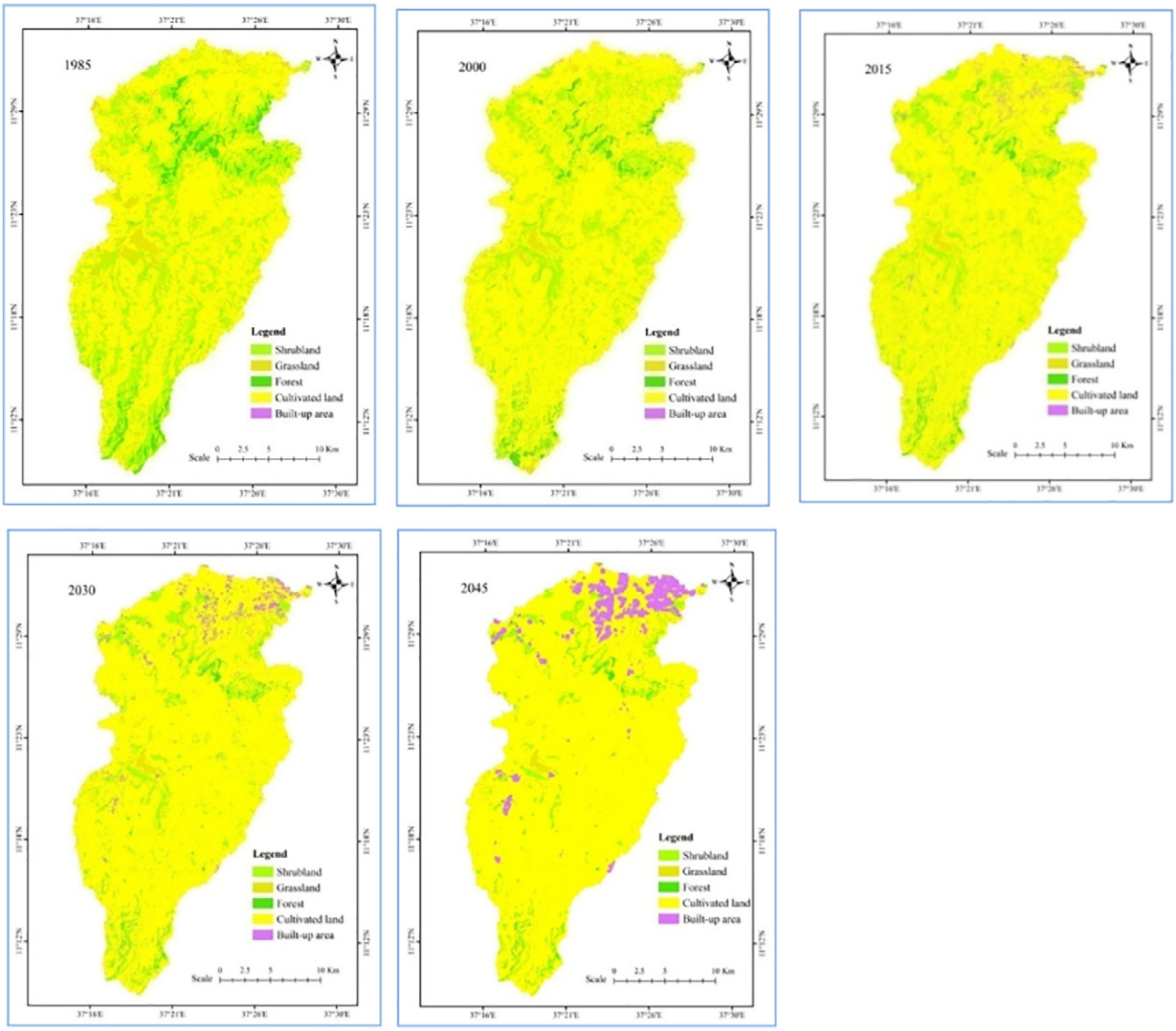

Fig. 5. LULC coverage in the Andassa watershed from 1985 to 2045 periods (Temesgen et al., 2017).

2.5.2.3. Soil. The physical and chemical properties of the soils in the watershed such as texture, available water content, hydraulic conductivity, bulk density and organic carbon content for different layers of each soil type are determining factors of runoff. According to FAO classification, there are 7 soil types in the study watershed. They are Haplic Alisols (49.6%), Eutric Leptosols (22.8%), Chromic Luvisols (10.8%), Haplic Nitisols (9%), Eutric Vertisols (7.1%), Eutric Regosols (0.6%) and Lithic Leptosols (0.2%) (Fig. 2). To account the soil properties in the model, a soil map was obtained from the hydrology department of EMWE. Related soil properties were also obtained from the Amhara National Regional State Bureau of Finance and Economic Development (ANRS BoFED). To integrate the soil map with the SWAT model, a soil database containing physical and chemical properties of soils was prepared for each soil layer and added to the SWAT soil databases.

2.5.2.4. Climate. SWAT requires long term daily climate data. Therefore, daily climate data for the periods 1990–2011 were collected from Bahir Dar (11. 6027°N, 37.322°E, 1827 m a.s.l), Adet (11.2745°N, 37.4931°E, 2179 m a.s.l) and Meshenti (11.47165°N, 37.2854°E, 1958 m a.s.l) meteorological stations, which were obtained from the Ethiopian National Meteorological Agency. The Meshenti station is within the watershed and only contains precipitation data. However, Bahir Dar and Adet stations contain all other climate variables such as precipitation, temperature (minimum and maximum), solar radiation, relative humidity and wind speed, and they are in the proximity of the watershed (Fig. 1). Dew points required for SWAT were then calculated for Bahir Dar and Adet stations using precipitation and temperature (minimum and maximum) data. Finally, the collected data were added into the SWAT weather database table. The mean monthly rainfall and temperature (1990–2011) characteristics of the stations are shown in Fig. 3.

2.5.2.5. Streamflow. The streamflow data, which was collected at the out let of the watershed (Fig. 1) for the periods 1990 to 2011, were used for calibration and validation of the SWAT model. The data was obtained from the hydrology department of EMWE.

2.5.3. Sensitivity analysis

Sensitivity analysis is a method of identifying the most important parameters for calibration and validation of SWAT model (Moriasi et al., 2007; Arnold et al., 2012a; Tang et al., 2012). To identify the most important SWAT parameters, 19 flow parameters (Table 1) were selected from literature (Tang et al., 2012; Gebremicael et al., 2013; Dila et al., 2016; Gyamfi et al., 2016; Khalid et al., 2016; Tekalegn et al., 2017). For this purpose, global sensitivity analysis (Abbaspour, 2013; Begou et al., 2016; Khalid et al., 2016), which allows changing each parameter at a time (Arnold et al., 2012a), was employed in SWAT-CUP 2012 version 5.1.4. Indices such as *t*-Stat and *p*-value were used to provide a measure and significance of sensitivity, respectively (Abbaspour, 2013; Narsimlu et al., 2015; Begou et al., 2016; Khalid et al., 2016). Hence, higher *t*-test in absolute values measures high sensitivity while a *p*-value of 0 is more significant (Abbaspour, 2013; Narsimlu et al., 2015; Khalid et al., 2016).

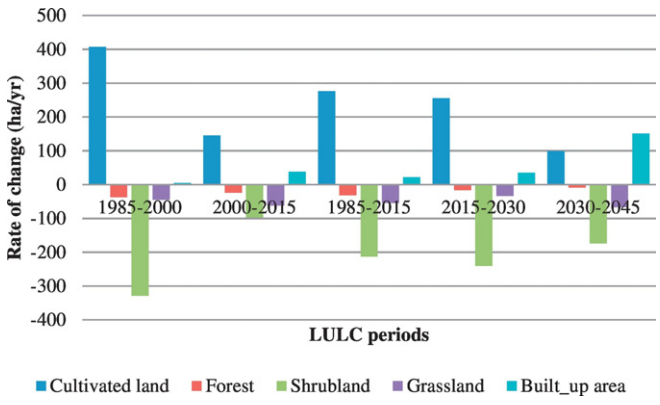

Fig. 6. Rate of LULC changes (ha/yr) from 1985 to 2045 periods in the Andassa watershed.

Table 2
Accuracy assessment of the 1985, 2000 and 2015 classified images.

		Reference from Google earth (Date: 05 February, 1985)					Row total	User acc. (%)
		CULT	FRST	SHRB	GRAS	BULT		
1985 classified image (Date:17 February, 1985)	CULT	152	1	2	17	2	174	87.4
	FRST	1	81	12	0	0	94	86.2
	SHRB	2	7	97	0	1	107	90.7
	GRAS	11	0	2	63	0	76	82.9
	BULT	3	0	0	2	24	29	82.8
	Column total	169	89	113	82	27	480	
	Prod. acc. (%)	89.9	91	85.8	76.8	88.9		
		Kappa coefficient = 0.83					Overall accuracy = 86.9%	
		Reference from Google earth (Date: 21 February, 2000)					Row total	User acc. (%)
		CULT	FRST	SHRB	GRAS	BULT		
2000 classified image (Date:03 February, 2000)	CULT	158	4	7	6	7	182	86.8
	FRST	3	67	6	1	0	77	87
	SHRB	6	3	89	5	0	103	86.4
	GRAS	11	0	0	61	2	74	82.4
	BULT	5	0	0	2	37	44	84.1
	Column total	183	74	102	75	46	480	
	Prod. acc. (%)	86.3	90.5	87.3	81.3	80.4		
		Kappa coefficient = 0.81					Overall accuracy = 85.8%	
		Reference from Google earth (Date: 28 February, 2015)					Row total	User acc. (%)
		CULT	FRST	SHRB	GRAS	BULT		
2015 classified image (Date: 20 February, 2015)	CULT	176	0	8	10	3	197	89.3
	FRST	0	54	2	0	0	56	96.4
	SHRB	0	5	87	2	0	94	92.6
	GRAS	6	0	5	60	2	73	82.2
	BULT	8	0	0	3	49	60	81.7
	Column total	190	59	102	75	54	480	
	Prod. acc. (%)	92.6	91.5	85.3	80	90.7		
		Kappa coefficient = 0.85					Overall accuracy = 88.8%	

Note: CULT, FRST, SHRB, GRAS, BULT are cultivated land, forest, shrubland, grassland and built-up area, respectively; Prod. acc. and User acc. are producer and user accuracy, respectively.

2.5.4. Calibration and validation

Model calibration is a procedure of altering or adjusting model parameters, within the recommended ranges, based on observed data to

Table 3
Sensitive flow parameters and their rank.

Parameter	*t*-Stat	*p*-Value	Rank of sensitivity	Fitted value	Min value	Max value
V_ALPHA_BF.gw	11.53	0.00	1	0.429	0.234	0.769
R_CN2.mgt[a]	2.92	0.00	2	−0.133	−0.185	−0.013
V_CH_K2.rte	2.25	0.02	3	106.4	63.7	128.4
V_GW_DELAY.gw	1.90	0.06	4	325.9	247.1	413.6
V_GWQMN.gw	1.50	0.13	5	2490.1	1852.6	3294.4
V_RCHRG_DP.gw	1.49	0.14	6	0.439	0.416	0.544
V_GW_REVAP.gw	1.16	0.25	7	0.017	0.005	0.035
V_ESCO.hru	0.77	0.44	8	0.907	0.882	0.948

Note: V implies replace the parameter with the fitted value; R indicate multiply the parameter with fitted value.
[a] Indicates adding 1 on the fitted value.

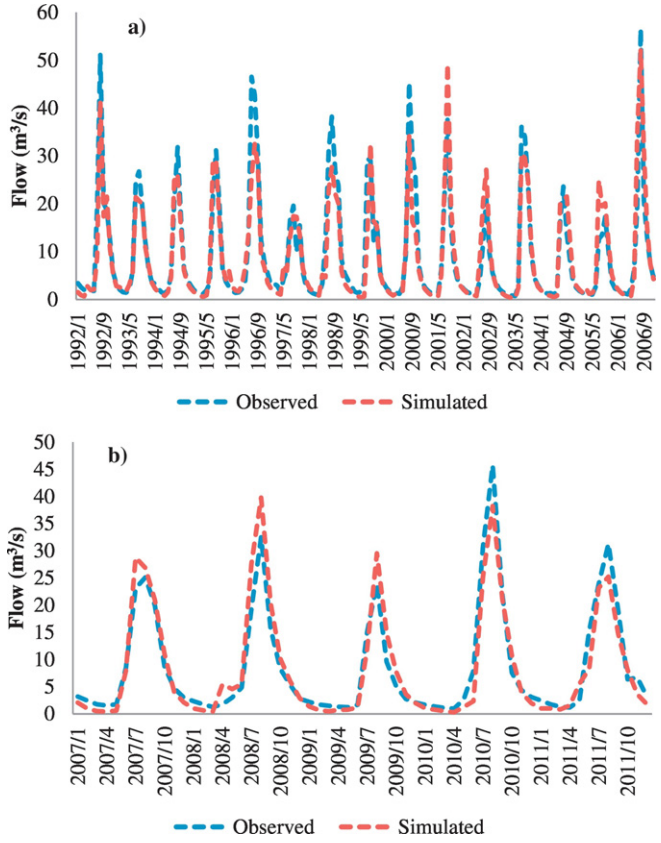

Fig. 7. Monthly average flow in the calibration (a) and validation (b) of the SWAT model.

ensure the same response over time (Lijalem et al., 2007; Arnold et al., 2012a; Vilaysane et al., 2015). On the other hand, validation is the process of checking the representation of the parameters by simulating the observed data with an independent data set without adjusting model parameters (Lijalem et al., 2007; Arnold et al., 2012a; Vilaysane et al., 2015). Therefore, in this study, calibration and validation were carried out using 22 years (1990–2011) of daily observed flow data. The data was divided into warm-up (1990–1991), calibration (1992–2006) and validation (2007–2011) periods. For a better parameterization of the SWAT model and to reduce the model output uncertainty, we have used a longer calibration period with a LULC data input within the calibration period (2000). Calibration and validation were carried out in SWAT-CUP 2012 version 5.1.4 using Sequential Uncertainty Fitting (SUFI-2) algorithm, based on the SWAT-CUP user manual (Abbaspour, 2013). SUFI-2 is a semi-automated calibration and uncertainty analysis algorithm (Zhou et al., 2014) that accounts for all sources of uncertainty, including uncertainty in the driving variables (e.g. rainfall), conceptual model, parameters and measured data (Tang et al., 2012; Zhou et al., 2014; Vilaysane et al., 2015). SUFI-2 is the most popular calibration and uncertainty analysis program and, has been used in many studies such as by Setegn et al. (2008) in the Lake Tana basin; Tang et al. (2012) in Chao river basin, China; Zhou et al. (2014) in Lake Dianchi basin, China; Narsimlu et al. (2015) in Kunwari river basin, India; Dila et al. (2016) in Gumera watershed, Ethiopia.

2.5.5. Model performance indices

There are various indices, which are available to check the performance of SWAT model. In this study, Nash–Sutcliffe Efficiency (NSE), Percent Bias (PBIAS) and Root Mean Square Error (RMSE)-observations standard deviation ratio (RSR) were used for evaluating the performance of the SWAT model as recommended by Moriasi et al. (2007). In addition to these indices, Coefficient of Determination (R^2), a measure of consistency of simulated and observed data, was also considered in evaluating the model. Therefore, the value of R^2 varies in between 0 and 1, where higher values indicate less error variance (Moriasi et al., 2007; Zhou et al., 2014; Ghoraba, 2015). NSE is a normalized statistics that determine the relative magnitude of the residual variance compared to the measured data variance. The values of NSE ranges from $-\infty$ to 1; in which higher value indicates the good performance of the model (Moriasi et al., 2007; Begou et al., 2016; Dila et al., 2016). PBIAS measures the estimation bias of the model. Positive and negative PBIAS indicated the underestimation and overestimation, respectively while low-magnitude values indicate better model simulations. The optimal value of PBIAS is 0 (Moriasi et al., 2007; Zhou et al., 2014; Begou et al., 2016; Gyamfi et al., 2016). RSR is the other commonly used error index statistics. RSR standardizes the RMSE using the observation standard deviations. The value of RSR ranges between 0 and a large positive number. The lower the RSR value is, the better the model simulation performance (Moriasi et al., 2007). The computation of R^2 is based on the formula available in Begou et al. (2016) and Tekalegn et al. (2017) while NSE, PBIAS (Moriasi et al., 2007; Tekalegn et al., 2017) and RSR

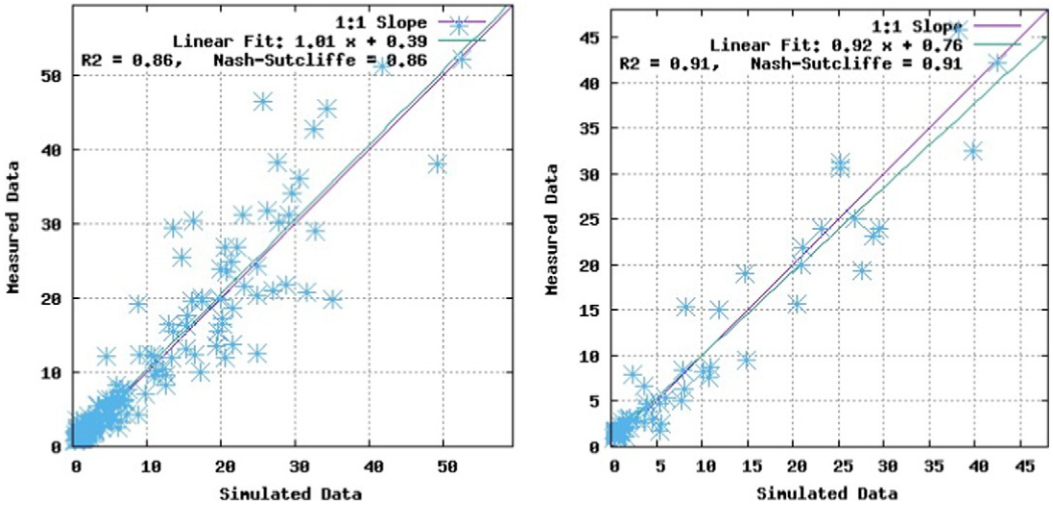

Fig. 8. Scatter plot of the observed (measured) and simulated monthly average flow (m^3/s) in the calibration (left) and validation (right) period.

Table 4
Model performance statistics for the calibration and validation periods.

Period	Evaluation statistics			
	R^2	NSE	PBIAS	RSR
Calibration	0.86	0.86	4.8	0.05
Validation	0.91	0.91	1.4	0.01

(Moriasi et al., 2007; Gyamfi et al., 2016) were calculated using Eqs. (6)–(8) respectively.

$$\mathrm{NSE} = 1 - \left[\frac{\sum_{i=1}^{n}\left(Y_i^{obs} - Y_i^{sim}\right)^2}{\sum_{i=1}^{n}\left(Y_i^{obs} - Y^{mean}\right)^2}\right] \quad (6)$$

$$\mathrm{PBAIS} = \left[\frac{\sum_{i=1}^{n}\left(Y_i^{obs} - Y_i^{sim}\right)^{*}100}{\sum_{i=1}^{n}\left(Y_i^{obs}\right)}\right] \quad (7)$$

$$\mathrm{RSR} = \frac{RMSE}{STD_{obs}} = \frac{\left[\sqrt{\sum_{i=1}^{n}\left(Y_i^{obs} - Y_i^{sim}\right)^2}\right]}{\left[\sqrt{\sum_{i=1}^{n}\left(Y_i^{obs} - Y^{mean}\right)^2}\right]} \quad (8)$$

where n is the total number of observations, Y_i^{obs} and Y_i^{sim} are the observed and the simulated value, respectively, Y^{mean} is the mean of the observed data and STD_{obs} is the standard deviation of the observed data.

2.5.6. Exploring the hydrological impacts of land use/land cover changes

Understanding the catchment response to LULC changes are important for water resources management measures (Nie et al., 2011; Yan et al., 2013; Huang and Lo, 2015; Gyamfi et al., 2016). To this effect, the classified (1985, 2000 and 2015) and the predicted (2030 and 2045) LULC maps were used to uncover the hydrologic impacts of LULC changes. The LULC maps were used separately while all other SWAT inputs were similar. A "*fixing-changing method*", meaning changing LULC maps keeping other inputs constant, was also employed by other studies such as by Nie et al. (2011) in the upper San Pedro watershed, Mexico; Yan et al. (2013) in Upper Du watershed, China; Huang and Lo (2015) in Yang Ming Shan National Park, Taiwan; Gyamfi et al. (2016) in Olifants basin, South Africa and Tekalegn et al. (2017) in Tana and Belese watersheds. The obtained hydrological components (e.g. annual flow, wet season flow, dry season flow, surface runoff, lateral flow, groundwater flow, water yield and ET) on annual and monthly average basis were, then compared. On the other hand, to assess the relation between changes in LULC classes and hydrological components, pairwise Pearson correlation (Nie et al., 2011; Yan et al., 2013; Tekalegn et al., 2017) were chosen and computed. Additionally, the hydrological impacts of individual LULC changes were explored using Partial Least Squares Regression (PLSR) model, which was done following the correlation analysis.

PLSR is an extension of multivariate analysis (Eq. 9), which generalizes and combines features from principal component analysis and multiple regressions (Abdi, 2007). PLSR predicts a set of dependent variable(s) from a set of independent variables (Wold et al., 2001; Abdi, 2007, 2010; Carrascal et al., 2009; Abdi et al., 2014). This prediction is achieved by extracting a set of latent factors (also named latent variables) that have the best predictive power (Abdi, 2007; Carrascal et al., 2009). PLSR is very useful under the following conditions: 1) when the numbers of predictors are similar or higher than observations, 2) for highly correlated predictors, 3) for a large number of predictors, and 4) for several response variables and many predictors (Wold et al., 2001; Carrascal et al., 2009; SAS Institute Inc., 2017). The presence of collinearity, a problem that exists due to a close relationship of independent variables, affects the predictive power of the dependent variables when one employs the ordinary multivariate analysis (Abdi, 2007; SAS Institute Inc., 2017). In this study, multicollinearity test of the independent variables (predictors) were employed, considering Tolerance and Variance Inflation Factor (VIF), and the result (not shown here) revealed the co-liner characteristics of the data. Obviously, VIF values above 10 and tolerance nearing to 0 indicate the presence of collinearity. Hence, for data showing collinearity like the case in the studied watershed, PLSR model is useful in exploring the individual variables' impacts (Abdi, 2007, 2010; Carrascal et al., 2009; Abdi et al., 2014; Godoy et al., 2014). PLSR model, though it was developed in areas of chemometrics, was also used in various environmental studies such as by Shi et al. (2013); Fang et al. (2015) and Tekalegn et al. (2017). The basic PLSR algorithm is not provided here, but can be found in Wold et al. (2001), Abdi (2007, 2010), Carrascal et al. (2009), Abdi et al. (2014) and Godoy et al. (2014).

$$y = b_0 + b_1x_1 + b_2x_2 + b_3x_3 + \ldots + b_ix_i \quad (9)$$

where y is the response variable, b_0 is the intercept, x is the independents variables from *1* to *i*, and b is the coefficients of the x variables.

The robust advantages of PLSR model are in that it gives weight for predictors by developing latent factors. Therefore, one can easily understand the most influencing variables for a particular response (Abdi, 2007). The dependent variables used in PLSR in this study were annual flow, wet season flow, dry season flow, surface runoff, lateral flow, groundwater flow, water yield and ET while the independent variables were the LULC classes. Considering their relationships, four PLSR models were developed for annual, wet season and dry season streamflow

Table 5
Annual average hydrological components (1992-2011) during the different LULC periods in the Andassa watershed.

	Streamflow (m^3/s)			Other hydrological components (mm)				
Study periods	Annual	Wet (June-September)	Dry season (Oct-May)	Surface runoff	Later flow	Ground water flow	Water yield	ET
1985	300.6	203.2	97.4	222.1	32.9	126.5	381.5	580.8
2000	304.5	208.5	96.0	233.7	31.0	121.9	386.6	579.0
2015	307.3	212.6	94.7	242.8	31.0	116.7	390.5	578.8
2030	312.4	219.2	93.2	258.1	28.2	110.5	396.7	577.1
2045	318.2	227.0	91.2	276.9	27.4	101.0	405.2	576.0
Percent changes (%)								
1985-2000	1.3	2.6	-1.4	5.2	-5.9	-3.7	1.3	-0.3
2000-2015	0.9	2.0	-1.4	3.9	0.2	-4.2	1.0	0.0
1985-2015	2.2	4.6	-2.8	9.3	-5.7	-7.8	2.4	-0.3
2015-2030	1.7	3.1	-1.6	6.3	-9.1	-5.4	1.6	-0.3
2030-2045	1.9	3.6	-2.1	7.3	-2.9	-8.6	2.1	-0.2

Note: ET = Evaporation and transpiration.

(PLSR 1), surface runoff and water yield (PLSR 2), lateral flow and groundwater flow (PLSR 3) and ET (PLSR 4). To overcome the problem of over fitting of the data, the appropriate number of predictors were determined using R^2 (goodness of fit), Q^2 (goodness of prediction) and Q^2_{cum} (cumulative goodness of prediction with a given number of factors) (Shi et al., 2013; Yan et al., 2013; Tekalegn et al., 2017). Generally, a Q^2_{cum} above 0.5 exhibits a good predictive ability of the PLSR model (Shi et al., 2013). In addition to these indices, Root Mean PRESS (Predicted Residual Sum of Squares) was used to determine the number of factors explaining the model (SAS Institute Inc., 2017). The "Statistically Inspired Modification of PLS" (SIMPLS) algorithm as recommended by De Jong (1993) for multiple response variables was chosen to estimate the response parameters. The detail procedures about the calculation R^2, Q^2 and Q_{cum} are available in SAS Institute Inc. (2017), Shi et al. (2013) and Yan et al. (2013). In PLSR, the Variable Importance for the Projection (VIP) represents the importance of the predictor in determining the PLS projection for both predictor and responses (Cox and Gaudard, 2013; Shi et al., 2013; SAS Institute Inc., 2017). Larger VIP values express the high importance of the variable (Shi et al., 2013). In general, a VIP value of 0.8 is considered as the minimum acceptable value in the wider scientific community (SAS Institute Inc., 2017). The regression coefficients in PLSR models were used to reveal the direction of the relationships between changes in individual LULC class and hydrological components (Shi et al., 2013; Yan et al., 2013). Though PLSR

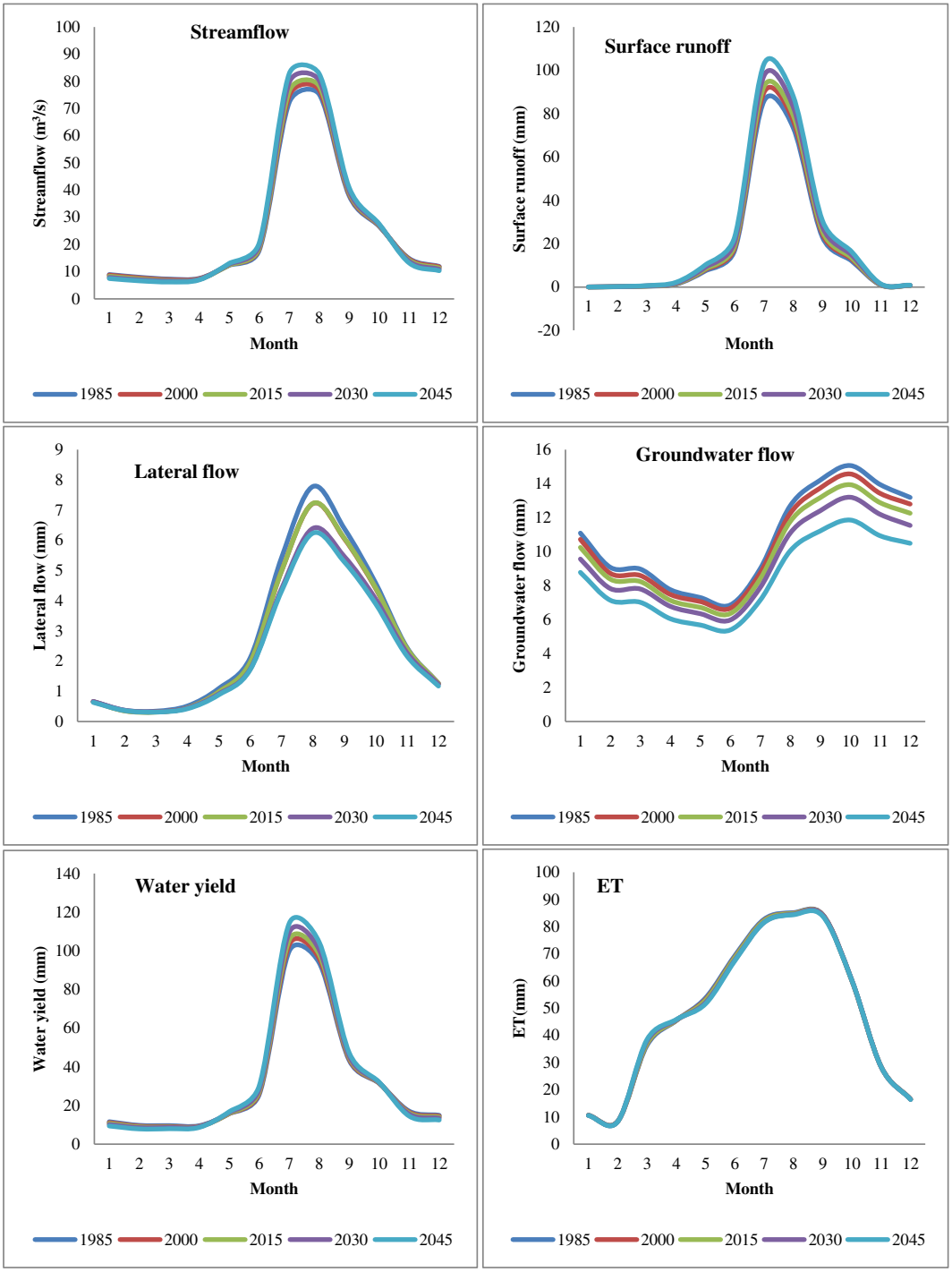

Fig. 9. Monthly average (1992–2011) streamflow, surface runoff, lateral flow, groundwater flow, water yield and ET response in the different LULC periods of the Andassa watershed.

Table 6
Pair-wise Pearson correlation for changes in five LULC types and hydrological components between the 1985 and 2045 periods.[a] Numbers in parenthesis are the probability values (*p*-value).

	CULT	FRST	SHRB	GRASS	BULT	Annual STQ	Wet STQ	Dry STQ	SUR Q	LAT Q	GW Q	WYLD	ET
CULT	1.000												
FRST	**−0.993**	1.000											
	(0.001)												
SHRB	**−0.992**	**0.977**	1.000										
	(0.001)	(0.004)											
GRAS	**−0.960**	**0.959**	**0.977**	1.000									
	(0.009)	(0.010)	(0.004)										
BULT	0.791	−0.766	−0.857	−0.913	1.000								
	(0.111)	(0.131)	(0.064)	(0.030)									
Annual STQ	**0.951**	**−0.931**	**−0.980**	**−0.988**	**0.937**	1.000							
	(0.013)	(0.022)	(0.003)	(0.002)	(0.019)								
Wet STQ	**0.953**	**−0.935**	**−0.981**	**−0.990**	**0.935**	**1.000**	1.000						
	(0.012)	(0.020)	(0.003)	(0.001)	(0.019)	(0.000)							
Dry STQ	**−0.959**	**0.946**	**0.983**	**0.995**	**−0.929**	**−0.998**	**−0.999**	1.000					
	(0.010)	(0.015)	(0.003)	(0.000)	(0.022)	(0.000)	(0.000)						
SUR Q	**0.947**	**−0.927**	**−0.977**	**−0.988**	**0.942**	**1.000**	**1.000**	**−0.998**	1.000				
	(0.015)	(0.023)	(0.004)	(0.002)	(0.017)	(0.000)	(0.000)	(0.000)					
LAT Q	**−0.963**	**0.929**	**0.981**	**0.945**	−0.855	**−0.974**	**−0.972**	**0.966**	**−0.971**	1.000			
	(0.008)	(0.023)	(0.003)	(0.015)	(0.065)	(0.005)	(0.006)	(0.007)	(0.006)				
GW Q	**−0.938**	**0.922**	**0.970**	**0.990**	**−0.951**	**−0.998**	**−0.999**	**0.998**	**−0.999**	**0.959**	1.000		
	(0.018)	(0.026)	(0.006)	(0.001)	(0.013)	(0.000)	(0.000)	(0.000)	(0.000)	(0.010)			
WYLD	**0.945**	**−0.926**	**−0.976**	**−0.989**	**0.946**	**1.000**	**0.999**	**−0.998**	**1.000**	**−0.967**	**−0.999**	1.000	
	(0.016)	(0.024)	(0.005)	(0.001)	(0.015)	(0.000)	(0.000)	(0.000)	(0.000)	(0.007)	(0.000)		
ET	**−0.978**	**0.952**	**0.995**	**0.968**	−0.877	**−0.985**	**−0.985**	**0.982**	**−0.983**	**0.992**	**0.974**	**−0.981**	1.000
	(0.004)	(0.013)	(0.000)	(0.007)	(0.051)	(0.002)	(0.002)	(0.003)	(0.003)	(0.001)	(0.005)	(0.003)	

[a] Bold numbers for $p < 0.05$, CULT: cultivated land; FRST: forest; SHRB: shrubland; GRAS: grassland; BULT: built-up area, STQ: streamflow; SUR Q: surface runoff; LAT Q: lateral flow; GW Q: groundwater flow; WYLD: water yield; ET: evaporation and transpiration.

does not rely on the distributional assumptions of normality (Cox and Gaudard, 2013; SAS Institute Inc., 2017), the data was also checked using the Shapiro–Wilk (S–W) (Shapiro and Wilk, 1965; Gyamfi et al., 2016; Tekalegn et al., 2017) normality test, and the result revealed that the data was from the normal distribution (Shapiro and Wilk, 1965) (see Appendix). PLSR was undertaken in JMP 13.2.0 while R statistical package version 3.3.2 (freely accessed from http://cran.r-project.org/) was employed for multicollinearity test of predictors and other statistics.

3. Results and discussion

3.1. Land use/land cover changes

The LULC states of the Andassa watershed between 1985 and 2045 periods are shown in Fig. 4 and Fig. 5. During 1985–2015, significant amount of LULC changes occurred in the watershed and, the changes are expected to continue in 2030 and 2045 periods. For example, cultivated land increased from 62.7% in 1985, to 73.1% in 2000, to 76.8% 2015, and continued increasing to 83.3% in 2030 and to 85.8% in 2045 periods (Fig. 4). Correspondingly, the extent of built-up areas were increased between 1985 and 2000 periods (0.1 to 0.2%), and the increment continued in 2015 (1.1%). It is expected to increase in the 2030 (2%) and 2045 (5.9%) periods (Fig. 4). The rapid percent change of built-up area during 1985–2000 and 2000–2015 periods were observed in the direction of the regional capital city Bahir Dar. Focus group discussions held with agricultural development agents are also consistent with this trend. For the study periods, however, the annual expansion rate (ha/yr) of cultivated land until 2030 is greater than built-up area (Fig. 6). Conversely, areas covered by forest deceased from 3.5% in 1985, to 2.6% in 2000, to 1.9% in 2015, and are expected to decrease to 1.5% and 1.3% in 2030 and 2045 periods, respectively (Fig. 4). Similarly, the extent of shrubland and grasslands were reduced throughout 1985, 2000 and 2015 periods, and expected to continue in 2030 and 2045 periods (Fig. 4). Though forest, shrubland and grassland experienced a reduction in converge throughout the study periods, the greatest reduction rate (ha/yr) was observed in shrubland (Fig. 6), which indicates that the expansion of cultivated land is utmost from shrubland. Population growth and reduction of land productivity are the drivers of such changes.

The finding of this study is consistent with other studies carried out by Kebrom and Hedlund (2000) in Kalu District, Abate (2011) in Borena Woreda, Rientjes et al. (2011) in Upper Gilgel Abbay catchment, Gebremicael et al. (2013) in Blue Nile basin and Temesgen et al. (2014) in Dera District, where cultivated land increased at the expense of reduction in forest and shrubland. The expansion of cultivated land and the shrinkage of forest were also reported by Gete and Hurni (2001) in Dembecha area; Solomon et al. (2010) in Koga watershed;

Table 7
Summary of PLSR models of the hydrological components in the Andassa watershed.

Response variable Y	R^2	Q^2	Component	% of explained variability in Y	Cumulative explained variability in Y (%)	Root Mean PRESS	Q^2 cum
Annual, Wet and Dry STQ	0.985	0.919	**1**	98.5	98.5	0.275	0.919
			2	1.1	99.6	0.334	0.990
			3	0.1	99.7	0.431	0.998
			4	0.3	100	0.431	0.999
			5	0.0	100	0.431	0.999
SUR Q and WYLD	0.996	0.989	1	97.9	97.9	0.311	0.903
			2	1.7	99.6	0.305	0.989
			3	0.2	99.8	0.402	0.998
			4	0.2	100	0.402	0.999
			5	0.0	100	0.402	0.999
LAT Q and GW QS	0.953	0.867	**1**	95.3	95.3	0.393	0.867
			2	1.3	96.6	0.627	0.987
			3	2.3	98.9	0.856	0.997
			4	1.1	100	0.856	0.999
			5	0.0	100	0.856	0.999
ET	0.999	0.999	1	97.4	97.4	0.261	0.932
			2	1.6	99.0	0.411	0.988
			3	0.9	99.9	0.258	0.999
			4	0.1	100	0.258	0.999
			5	0.0	100	0.258	0.999

Note: The bold number indicated the number of factors required to fit the PLSR models; the minimum Root Mean PRESS shows the number of predictors explain the model (SAS Institute Inc, 2017).

Table 8
VIP values and PLSR weights of hydrological components in the Andassa watershed.

PLSR Predictors	Annual, wet and dry STQ		SUR Q and WYLD			LAT Q and GW Q		ET			
	VIP	W*(1)	VIP	W*(1)	W*(2)	VIP	W*(1)	VIP	W*(1)	W*(2)	W*(3)
CULT	0.994	**+0.445**	0.985	**+0.443**	**−0.309**	1.006	**−0.450**	1.019	**−0.458**	**−0.821**	**+0.457**
FRST	0.977	**−0.437**	0.970	**−0.433**	**+0.458**	0.979	**+0.438**	0.997	**+0.446**	**−0.717**	**+1.127**
SHRB	1.022	**−0.457**	1.012	**−0.457**	+0.073	1.032	**+0.462**	1.049	**+0.466**	**+1.218**	**−1.066**
GRAS	1.033	**−0.462**	1.025	**−0.462**	−0.076	1.025	**+0.458**	1.019	**+0.453**	**−1.139**	**+0.991**
BULT	0.973	**+0.435**	1.008	**+0.442**	**+0.832**	0.956	**−0.428**	0.910	**−0.411**	+0.209	**+0.643**

Note: The bold numbers are values greater than 0.3, the positive and negative signs indicate the sign of the loadings in PLSR model.

Ariti et al. (2015) in Central Rift Valley and Ebrahim and Mohamed (2017) in Geleda catchment. The increase of built-up area in this watershed study also coincides with other research findings in Ethiopia (such as Gete and Hurni (2001) in Dembecha area; Belay (2002) in Derekolli catchment; Getachew and Melesse (2012) in Angereb watershed) and elsewhere (such as Gyamfi et al. (2016) in Olifants basin, South Africa and Karamage et al. (2017) in Rwanda).

3.2. Accuracy assessment and CA-Markov validation

The accuracy report of the three classified images is shown in Table 2. Overall accuracy of the classification ranges between 85.8% and 88.8% for the period 1985, 2000 and 2015. A Kappa coefficient of above 0.80 was also obtained for the three classified images. According to Monserud (1990), Kappa values between 0.70 and 0.85 are very good indicators of the classified image. Therefore, the validation data set indicated a very good agreement of the classified image with the ground truths.

Validation of CA-Markov was performed, and a ROC value of 89.5% was achieved. The Kappa statistics such as *K*no (87.7%), *K*location (82.2%), *K*locationStrata (82.2%) and *K*standard (81.6%) were also above 80%, which indicates the good performance of the model in simulating the 2030 and 2045 LULC status (Singh et al., 2015; Mosammam et al., 2016). The detail discussions of CA-Markov validation are available in Temesgen et al. (2017).

3.3. Sensitive SWAT parameters

Sensitivity analysis, which was carried out using 19 flow parameters (Table 1), identified the 8 most sensitive parameters controlling the output variable (Table 3). The three most sensitive parameters in the order of sensitivity are ALPHA_BF.gw, CN2.mgt and CH_K2.rte.These parameters are highly related to surface runoff. Additionally, the parameters ALPHA_BF.gw and CN2.mgt were also identified as the most sensitive parameters in the region (Gebremicael et al., 2013; Dila et al., 2016).

Table 9
PLSR coefficients showing the impacts of individual LULC types on hydrological components during 1985 to 2045 periods.

PLSR model	Response variables	PLSR predictors				
		Cultivated land	Forest	Shrubland	Grassland	Built-up area
PLSR 1	Annual STQ	+0.2036	−0.1999	−0.2092	−0.2114	+0.1992
	Wet STQ	+0.2039	−0.2003	−0.2096	−0.2118	+0.1995
	Dry STQ	−0.2046	+0.2010	+0.2103	+0.2125	−0.2002
PLSR 2	SUR Q	+0.1301	−0.0912	−0.1918	−0.2291	+0.3963
	WYLD	+0.1254	−0.0844	−0.1907	−0.2302	+0.4086
PLSR 3	LAT Q	−0.2010	+0.1956	+0.2062	+0.2047	−0.1911
	GW Q	−0.2051	+0.1997	+0.2104	+0.2089	−0.1950
PLSR 4	ET	−0.5893	−0.2916	+0.8638	−0.4008	−0.2605

Note: The positive and negative signs revealed the position of influence.

3.4. Calibration and validation

The graphical comparison of observed and simulated flow for the calibration (1992–2006) and validation (2007–2011) periods are shown in Fig. 7 and Fig. 8. The simulation has captured the observed flow reasonably. Statistical performance indices are also shown in Table 4. The obtained R^2 (0.86 for calibration and 0.91 for validation) values show very good consistency between the observed and simulated data, and indicates less error variance between the two data (Moriasi et al., 2007; Begou et al., 2016; Gyamfi et al., 2016; Tekalegn et al., 2017). NSE above 0.75, PBAIS < 10% and RSR < 0.5 were also attained. The positive values of PBAIS indicate the under estimation of the model. According to Moriasi et al. (2007), the performance of the model is very good. The overall performance indices during the validation period are higher than the performance indices of calibration period, which suggests an overall superior quality of data. Similar model efficiency improvements in the validation period were also reported by Uhlenbrook et al. (2010) and Nie et al. (2011). In general, the performance indices obtained during the calibration and validation periods indicated a very good performance rate of the model in simulating the hydrological impacts of LULC changes over the 1985 to 2045 periods.

3.5. Hydrological impacts of land use/land cover changes at the watershed scale

The impacts of LULC changes on streamflow in the Andassa watershed are summarized in Table 5. Corresponding to the increase of cultivated land and built-up area and the reduction of forest, shrubland and grassland (Fig. 4), the annual streamflow of the watershed has increased from 300.6 mm in 1985 to 304.5 mm in 2000 and to 307.3 mm in 2015. The continued increase of cultivated land and built-up area and extraction of vegetation covers (Fig. 4) are expected to further increase the annual streamflow in the 2030 (312.4 mm) and 2045 (318.2 mm) periods. A similar increment in response to the LULC changes was also observed in the wet season flow (June–September) throughout the 1985 to 2045 periods (203.2 mm, 208.5 mm, 212.6 mm, 219.2 mm and 227 mm in 1985, 2000, 2015, 2030 and 2045, respectively). Conversely, the reduction of vegetation covers and the increase of cultivated land and built-up area have reduced the dry season flow over these periods (97.4 mm, 96 mm, 94.7 mm, 93.2 mm and 91.2 mm in 1985, 2000, 2015, 2030 and 2045 LULC, respectively).

The finding of this study is consistent with several studies. For example, the increasing trend of annual, wet (June–September) and short (March–May) rainy season streamflow and, the decreasing trend of dry season flow (October–February) at El Diem station of Blue Nile basin during the 1970–2010 periods were associated with the conversion of vegetation cover into agriculture and grasslands over large areas of the basin (Gebremicael et al., 2013). A study in Angereb watershed also revealed the increase of mean wet monthly flow (39%) and decrease of dry average monthly flow (46%) due to the conversion of

forest to agriculture between the 1985 and 2011 periods (Getachew and Melesse, 2012). The increase of streamflow in Quaternary Catchment, South Africa during the 2004–2013 periods was also due to the increased of cultivated land (92%) and the reduction of wooded land (35%) and grasslands (9.8%) (Gwate et al., 2015). Similarly, the significant decline of minimum daily flows in the Chemoga watershed during the three driest months (December to February) between the 1960 and 1999 periods was partially explained by changes in LULC and degradation of the watershed that involves destruction of natural vegetative covers, expansion of croplands, overgrazing and increased area under eucalyptus plantations (Woldeamlak and Sterk, 2005). Likewise, the reduction of low flow index in the Upper Gilgel Abbay catchment was also due to the expansion of agricultural land at the expense of forest lands and changes in the annual and seasonal distribution of rainfall (Rientjes et al., 2011). Koch et al. (2012) also indicated that the transition towards artificial land use in Gedeb catchment at the cost of the natural landscape causes higher overland flows. In the same way, Tekleab et al. (2013) also explained the situation in the same catchment as enhanced peak discharge during the 1973–2010 periods was typically associated with the LULC changes in the catchment.

The impacts of LULC changes on the annual average surface runoff, lateral flow, groundwater flow, water yield and ET are provided in Table 5. Correspondingly, the increase of cultivated land and built-up area and the reduction of vegetation types of LULC (Fig. 4) have resulted in a surface runoff increase from 221.1 mm in 1985 to 233.7 mm in 2000 and, to 242.8 mm in 2015. The increment in surface runoff is also expected to continue into 2030 (258.1 mm) and 2045 (276.9 mm) LULC periods. Similarly, water yield has increased throughout the 1985 to 2045 LULC periods (381.5 in 1985, 386.6 in 2000, 390.5 in 2015, 396.7 in 2030 and 405.2 in 2045). In contrast, groundwater flow has reduced through the 1985 (126.5 mm), 2000 (121.9 mm), 2015 (116.7 mm), 2030 (110.5 mm), and 2045 (101 mm) periods. Similarly, lateral flow has reduced from 32.9 mm in 1985 to 31 mm in 2000 and, will continue its reduction to 28.2 mm in 2030 and to 27.4 mm in 2045 LULC. The reduction of ET has also been observed through 1985 to 2045 periods (580.8 mm, 579 mm, 578.8 mm, 577.1 mm and 576 mm in 1985, 2000, 2015, 2030 and 2045, respectively), though the change is not considerable (Table 5). The effects of LULC changes on streamflow, surface runoff, water yield, groundwater flow and lateral flow are clearly seen in both the annual and monthly average values. Conversely, the influence of LULC on ET is very small especially on the monthly average values (Fig. 9). Over 1985 to 2045 periods, water yield has increased from June to September, and shows a reduction in the rest of the months (Fig. 9). The increase of water yield over these periods is, therefore, due to the increase of water yield in the four wet months (June–September). Hence, the reduction of water yield in driest months (October–May) is attributed to the reduction of flow in these months.

The findings of this study are consistent with various research findings such as Gyamfi et al. (2016) in Olifants basin, South Africa and Tekalegn et al. (2017) in Lake Tana catchment and Beles watershed, Ethiopia, where cultivated lands are increased at the expense of vegetation covers, and where surface runoff is increased and groundwater flow reduced. Nie et al. (2011) also reported that the overall increase of surface runoff between the 1973 to 1997 periods in the upper San Pedro watershed, Mexico was attributed to the increase of urban, agriculture and woody mosquite, and the decrease of grassland and desert scrub. The increment of surface runoff due to the expansion of cultivated land and urbanization at the expense of vegetation covers were also reported by Karamage et al. (2017) in Rwanda. Due to the significant decrease of forest, shrubland and grassland due to the cultivated land and built-up area, the decrease of ET in the studied watershed is expected (although the change is insignificant). Therefore, the result of this study is generally in agreement with the fact that seasonal crops (here cultivated land) have less ET than perennial trees (here vegetative LULC) (Yan et al., 2013; Deng et al., 2015; Tekalegn et al., 2017).

3.6. Hydrological impacts of individual land use/land cover changes

The pair-wise association of the five LULC classes and hydrological components is shown in Table 6. The result indicated that almost all LULC classes have a strong association with the different hydrological components. For example, forest has a significant negative correlation with annual flow, wet season flow, surface runoff and water yield while its correlation with dry season flow, lateral flow, groundwater flow and ET are positive (Table 6). In the same pattern, shrubland has significantly correlated with annual flow ($r = -0.980$), wet season flow ($r = -0.981$), dry season flow ($r = 0.983$), surface runoff ($r = -0.977$), lateral flow ($r = 0.981$), groundwater flow ($r = 0.970$), water yield ($r = -0.976$) and ET ($r = 0.995$). Correspondingly, grassland has a significant correlation with annual flow ($r = -0.988$), wet season flow ($r = -0.990$), dry season flow ($r = 0.995$), surface runoff ($r = -0.988$), lateral flow ($r = 0.945$), groundwater flow ($r = 0.990$), water yield ($r = -0.989$) and ET ($r = 0.968$). It is also observed that cultivated land has significantly correlated with annual and wet season flow (positive), dry season flow (negative), lateral flow (negative), groundwater flow (negative) and ET (negative) (Table 6). However, built-up area has no significant association with lateral flow and ET while it has significant correlation with other hydrologic components (Table 6). The significant correlation of almost all LULC classes with most studied hydrological components suggests that almost all LULC classes are very important for the changes in hydrological components.

Significant correlations among hydrological components were also observed in the study watershed (Table 6). Importantly, the correlation between annual flow, surface runoff and water yield are perfectly positive while they are negatively correlated with dry season flow, lateral flow, groundwater flow and ET. The result has also indicated that the correlation among dry season flow, lateral flow, groundwater flow and ET are positively significant. Above all, the significant correlation among hydrological components supports the general idea that the increment of one hydrological component increases the quantity of some other components, while reducing the amount of other components. Similar to the results observed in this study, an increase in surface runoff and water yield and a reduction of groundwater flow were also observed in Olifants basin, South Africa (Gyamfi et al., 2016) and in the upper San Pedro watershed, Mexico (Nie et al., 2011) between 2000 and 2013 and, the 1973–1992 periods respectively.

A summary of the four PLSR models constructed separately are given in Table 7. In the four PLSRs models such as in PLSR 1 (annual, wet season and dry season flow), PLSR 2 (surface runoff and water yield), PLSR 3 (lateral flow and groundwater flow) and PLSR 4 (ET), the obtained R^2 and Q^2_{cum} values are above 0.50, suggesting a good prediction of the models. For annual, wet season and dry season flow, one component explains the model (98.5% of the variation). Addition of other factors does not considerably improve the prediction capacity of the model, at the same time it does not substantially enhance the percent variation explained by predictors (Table 7). Inclusion of other factors, rather, increase prediction error. The increase of prediction error with the addition of more predictors suggests that other predictors are not strongly correlated with the residual of the predicted variables. The first PLSR model is dominated by cultivated land and built-up area on the positive side and forest, shrubland and grassland on the negative side. To distinguish the relative importance of predictors, shrubland and grassland (VIP > 1.0) has more significance in this model (Table 8). The regression coefficients also express that cultivated and built-up area influence annual and wet season flow positively while the effects of forest, shrubland and grassland on these components are negative. Conversely, the influence of cultivated land and built-up area on dry season flow is negative and the vegetative LULC affects dry season flow positively (Table 9).

For surface runoff and water yield (PLSR 2), two components explain the model, which accounts 99.6% of the variations. Adding the third component does not considerably improve the predictive ability of the model and percent variation explained by predictors (Table 7). The result disclosed that changes in surface runoff and water yield were dependent on cultivated land and built-up area (on the positive side) and forest, shrubland and grassland (on the negative side), from which shrubland, grassland and built-up area have relatively greater importance (VIP > 1.0) in this model (Table 8). The regression coefficients of this model have also provided a similar direction of influences as discussed above (Table 9). For lateral flow and groundwater (PLSR 3), a single component has explained the model, which accounts 95.3% of the variations explained by predictors. Again, adding other predictors does not noticeably improve model prediction and percent variations explained by predictors (Table 7). The LULC categories that explain the variance in lateral flow and groundwater flow on the positive and negative side are forest, shrubland and grassland, and cultivated land and built-up area, respectively (Table 8). A similar direction of influence by predictors on lateral flow and groundwater flow is also expressed by the regression coefficients (Table 9). The close association of decrease in lateral flow and groundwater and reduction of vegetation covers, suggest that the reduction of vegetation covers reduced lateral flow and groundwater flow in the study watershed. In the fourth PLSR model (ET), the minimum Root Mean PRESS was obtained with three components, which explains 99.9% of the variance (Table 7). Among the LULC classes, cultivated land, shrubland and grassland have greater importance (VIP > 1) for the small change in it (Table 8). In this model, cultivated land, forest, grassland and built-up area have negative regression coefficients. In contrast, shrubland has a positive regression coefficient (Table 9).

4. Conclusions

This study clearly indicated the effects of LULC changes on the hydrology of the Andassa watershed. The expansions of cultivated and built-up area and the withdrawing of forest, shrubland and grassland during the 1985 to 2015 periods had increased the annual and wet season flow, surface runoff and water yield. In contrast, the LULC changes had decreased dry season flow, groundwater flow, lateral flow and ET. The 2030 and 2045 LULC states are expected to further increase the annual and wet season flow, surface runoff and water yield, and reduce dry season flow, groundwater flow, lateral flow and ET. The effects of LULC changes on streamflow, surface runoff, groundwater flow, lateral flow and water yield are very significant in both the annual and monthly average values. Nevertheless, the LULC change effect on ET is very small especially in the monthly average values. It was found that the changes in cultivated land, forest, shrubland, grassland and built-up area have different contribution for the changes in annual and wet season flow, dry season flow, and to the different water balance components. The expected increase of wet season flow may result flooding, and the reduction of dry season flow may affect future irrigation practice. Additionally, the increase of runoff may also have a wider implication for increasing soil erosion and sedimentation unless the proper management is not be implemented. Therefore, curving the trends of LULC towards increasing vegetation covers is very important in order to reduce the wet season flow and surface runoff and, increase the dry season flow, lateral flow and groundwater flow. One way of increasing vegetation cover in the study watershed is through changing the widely implemented cereal production with fruits. Moreover, proper soil and water conservation measures are highly necessary.

Acknowledgement

The Authors are very much grateful to acknowledge Center for Environmental Science, Addis Ababa University and Adigrat University for financial support; Ministry of Water and Energy for providing GIS and hydrology data; Amhara National Regional State Bureau of Finance and Economic Development (ANRS BoFED) for providing the soil data; Ethiopian Meteorological Agency for providing climate data; agricultural development agents and local elders of the watershed for their interest to focus group discussions and providing necessary information. We are also very delighted to acknowledge the efforts of the two anonymous reviewers and the editor for the substantial improvement of the paper.

Appendix A. Supplementary data

Supplementary data to this article can be found online at https://doi.org/10.1016/j.scitotenv.2017.11.191.

References

Abate, S., 2011. Evaluating the land use and land cover dynamics in Borena Woreda of South Wollo highlands, Ethiopia. J. Sustain. Dev. Afr. 13 (1), 87–105.
Abbaspour, K., 2013. SWAT-CUP 2012: SWAT Calibration and Uncertainty Programs — A User Manual 103 pp.
Abdi, H., 2007. Partial least square regression (PLS regression). In: Salkind, N.J. (Ed.), Encyclopedia of Measurement and Statistics. Sage Publications, Thousand Oaks, CA.
Abdi, H., 2010. Partial least squares regression and projection on latent structure regression (PLS Regression). WIREs Comput. Stat. 2 (1), 97–106.
Abdi, H., Bastien, P., Vinzi, V., Tenenhaus, M., Carrascal, L., Galván, I., Eriksson, L., 2014. Partial least squares regression and projection on latent structure regression. Chemom. Intell. Lab. Syst. 2 (2), 3925–3942.
Ariti, A., Vliet, J., Verburg, P., 2015. Land-use and land-cover changes in the Central Rift Valley of Ethiopia: assessment of perception and adaptation of stakeholders. Appl. Geogr. 65, 28–37.
Arnold, J., Srinivason, R., Muttiah, R., Williams, J., 1998. Large area hydrologic modeling and assessment. Part I: model development. J. Am. Water Resour. Assoc. 34 (1), 73–89.
Arnold, J., Kiniry, J., Srinivasan, R., Williams, J., Haney, E., Neitsch, S., 2011. Soil and Water Assessment Tool. Input/Output File Documentation Version 2009 Texas Water Resources Institute Technical Report No. 365. 643 pp.
Arnold, J., Moriasi, D., Gassman, P., Abbaspour, K., White, M., Srinivasan, R., Santhi, C., Harmel, R., van Griensven, A., Van Liew, M., Kannan, N., Jha, M., 2012a. SWAT: model use, calibration, and validation. Trans. ASABE 55 (4), 1491–1508.
Arnold, J., Kiniry, J., Srinivasan, R., Williams, J., Haney, E., Neitsch, S., 2012b. Soil and Water Assessment Tool. Input/Output Documentation Version 2012. Texas Water Resources Institute TR-439. 654 pp.
Arsanjani, J., Kainz, W., Mousivand, A., 2011. Tracking dynamic land-use change using spatially explicit Markov Chain based on cellular automata: the case of Tehran. Int. J. Image Data Fusion. https://doi.org/10.1080/19479832.2011.605397.
Begou, J., Jomaa, S., Benabdallah, S., Bazie, P., Afouda, A., Rode, M., 2016. Multi-site validation of the SWAT model on the Bani catchment: Model performance andpredictive uncertainty. Water 8, 178.
Belay, T., 2002. Land-cover/land-use changes in the Derekolli catchment of the South Welo Zone of Amhara Region, Ethiopia. East. Afr. Soc. Sci. Res. Rev. 18 (1), 1–20.
Boakye, E., Odai, S., Adjei, K., Annor, F., 2008. Landsat images for assessment of the impact of land use and land cover changes on the Barekese Catchment in Ghana. Eur. J. Sci. Res. 22 (2), 269–278.
Bongers, F., Alemayehu, W., Sterck, F., Tesfaye, B., Demel, T., 2006. Ecological restoration and church forests in northern Ethiopia. J. Drylands 1 (1), 35–44.
Carrascal, L., Galván, I., Gordo, O., 2009. Partial least squares regression as an alternative to current regression methods used in ecology. Oikos 118 (5), 681–690.
Clark Labs, 2012. Idrisi Selva Help System. Clark University, USA.
Cox, I., Gaudard, M., 2013. Discovering Partial Least Squares with JMP®. SAS Institute, Inc., Cary, North Carolina, USA.
De Jong, S., 1993. SIMPLS: an alternative approach to partial least squares regression. Chemom. Intell. Lab. Syst. 18, 251–263.
Deng, Z., Zhang, X., Li, D., Pan, G., 2015. Simulation of land use/land cover change and its effects on the hydrological characteristics of the upper reaches of the Hanjiang Basin. Environ. Earth Sci. 73, 1119–1132.
Dila, Y., Daggupati, P., George, C., Srinivasan, R., Arnold, J., 2016. Introducing a new open source GIS user interface for the SWAT model. Environ. Model. Softw. 85, 129–138.
Eastman, J., 2012. IDRISI Selva Manual, Version 17. Clark University 322 pp.
Easton, Z., Fuka, D., White, E., Collick, A., Ashagre, B., McCartney, M., Awulachew, S., Ahmed, A., Steenhuis, T., 2010. A multi basin SWAT model analysis of runoff and sedimentation in the Blue Nile, Ethiopia. Hydrol. Earth Syst. Sci. 14, 1827–1841.
Ebrahim, E., Mohamed, A., 2017. Land use/cover dynamics and its drivers in Gelda catchment, Lake Tana watershed, Ethiopia. Environ. Syst. Res. 6 (4), 1–13.
Fang, N., Shi, Z., Chen, F., Wang, Y., 2015. Partial least squares regression for determining the control factors for runoff and suspended sediment yield during rainfall events. Water 7 (7), 3925–3942.
Fu, B., Chen, L., Ma, K., Zhou, H., Wang, J., 2000. The relationships between land use and soil conditions in the hilly area of the Loess Plateau in northern Shaanxi, China. Catena 36, 69–78.

Gebremicael, T., Mohamed, Y., Betrie, G., van der Zaag, P., Teferi, E., 2013. Trend analysis of runoff and sediment fluxes in the Upper Blue Nile basin: a combined analysis of statistical tests, physically-based models and land use maps. J. Hydrol. 482, 57–68.
Gessesse, D., Kleman, J., 2007. Pattern and magnitude of deforestation in the South Central Rift Valley Region of Ethiopia. Mt. Res. Dev. 27, 162–168.
Getachew, H., Melesse, A., 2012. The impact of land use change on the hydrology of the Angereb watershed, Ethiopia. Int. J. Water Sci. 1 (4), 1–7.
Gete, Z., Hurni, H., 2001. Implications of land use and land cover dynamics for mountain resource degradation in the northwestern Ethiopian Highlands. Mt. Res. Dev. 21 (2), 184–191.
Ghoraba, S., 2015. Hydrological modeling of the Simly Dam watershed (Pakistan) using GIS and SWAT model. Alex. Eng. J. 54, 583–594.
Girmay, G., Singh, B., Nyssen, J., Borrosen, T., 2009. Runoff and sediment-associated nutrient losses under different land uses in Tigray, Northern Ethiopia. J. Hydrol. 376, 70–80.
Githui, A., Mutua, F., Bauwens, W., 2009. Estimating the impacts of land-cover change on runoff using the soil and water assessment tool (SWAT): case study of Nzoia catchment, Kenya. Hydrol. Sci. J. 54 (5), 899–908.
Godoy, J., Vega, J., Marchetti, J., 2014. Relationships between PCA and PLS-regression. Chemom. Intell. Lab. Syst. 130, 182–191.
Green, W., Ampt, G., 1911. Studies on soil physics: part I. The flow of air and water through soils. J. Agric. Sci. 4, 1–24.
Gwate, O., Woyessa, Y., Wiberg, D., 2015. Dynamics of land cover and impact on streamflow in the Modder River Basin of South Africa: case study of a Quaternary catchment. Int. J. Environ. Prot. Pol. 3 (2), 31–38.
Gyamfi, C., Ndambuki, J., Salim, R., 2016. Hydrological responses to land use/cover changes in the Olifants basin, South Africa. Water 8:588. https://doi.org/10.3390/w8120588.
Huang, T., Lo, K., 2015. Effects of land use change on sediment and water yields in Yang Ming Shan National Park, Taiwan. Environments 2, 32–42.
Hurni, H., Kebede, T., Gete, Z., 2005. The implications of changes in population, land use, and land management for surface runoff in the Upper Nile Basin area of Ethiopia. Mt. Res. Dev. 25 (2), 147–154.
Karamage, F., Zhang, C., Fang, X., Liu, T., Ndayisaba, F., Nahayo, L., Kayiranga, A., Nsengiyumva, J., 2017. Modeling rainfall-runoff response to land use and land cover changes in Rwanda (1990–2016). Water 9:147. https://doi.org/10.3390/w9020147.
Kebrom, T., Hedlund, L., 2000. Land cover changes between 1958 and 1986 in Kalu District, Southern Wello, Ethiopia. Mt. Res. Dev. 20 (1), 42–51.
Khalid, K., Ali, M., Rahman, N., Mispan, M., Haron, S., Othman, Z., Bachok, M., 2016. Sensitivity analysis in watershed model using SUFI-2 algorithm. Proc. Eng. 162, 441–447.
Kidane, W., Bogale, G., 2017. Effect of land use land cover dynamics on hydrological response of watershed: case study of Tekeze Dam watershed, northern Ethiopia. Int. Soil Water Conserv. Res. 5, 1–6.
Koch, F., Griensven, A., Uhlenbrook, S., Tekleab, S., Teferi, E., 2012. The effects of land use change on hydrological responses in the Choke Mountain Range (Ethiopia) — a new approach addressing land use dynamics in the model SWAT. 2012 International Congress on Environmental Modeling and Software, Leipzig, Germany.
Kushwaha, A., Jain, M., 2013. Hydrological simulation in a forest dominated watershed in Himalayan region using SWAT model. Water Resour. Manag. 27, 3005–3023.
Lambin, E., Geist, H., Lepers, E., 2003. Dynamics of land use and land cover change in tropical regions. Annu. Rev. Environ. Resour. 28, 206–232.
Li, S., Jin, B., Wei, X., Jiang, Y., Wang, J., 2015. Using CA-Markov model to model the spatiotemporal change of land use/cover in Fuxian Lake for decision support. International Workshop on Spatiotemporal Computing, 13–15 July 2015, Fairfax, Virginia, USA.
Lijalem, Z., Roehrig, J., Dilnesaw, A., 2007. Calibration and validation of SWAT hydrologic model for Meki watershed, Ethiopia. Conference on International Agricultural Research for Development. University of Kassel-Witzenhausen and University of Göttingen, October 9–11, 2007.
MEA (Millennium Ecosystem Assessment), 2005. Ecosystems and Human Well-being: Synthesis. Island Press, Washington, DC.
Monserud, R., 1990. Methods for Comparing Global Vegetation Maps, Report WP-90-40. IIASA, Laxenburg.
Moriasi, D., Arnold, J., Van Liew, M., Bingner, R., Harmel, R., Veith, T., 2007. Model evaluation guidelines for systematic quantification of accuracy in watershed simulations. ASABE 50 (3), 885–900.
Mosammam, H., Nia, J., Khani, H., Teymouri, A., Kazem, M., 2016. Monitoring land use change and measuring urban sprawl based on its spatial forms: the case of Qom city. Egypt. J. Remote Sens. Space Sci. https://doi.org/10.1016/j.jrs.2016.08.002.
Narsimlu, B., Gosain, A., Chahar, B., Singh, S., Srivastava, P., 2015. SWAT model calibration and uncertainty analysis for streamflow prediction in the Kunwari River Basin, India, using sequential uncertainty fitting. Environ. Process. 2, 79–95.
Neitsch, S., Arnold, J., Kiniry, J., Williams, J., King, K., 2002. Soil and Water Assessment Tool Theoretical Documentation Version 2000. Texas Water Resources Institute, College Station, Texas TWRI Report TR-191. 458 pp.
Neitsch, S., Arnold, J., Kiniry, J., Williams, J., 2011. Soil and Water Assessment Tool Theoretical Documentation Version 2009 Texas Water Resources Institute Technical Report No. 406. 618 pp.
Neupane, R., Kumar, S., 2015. Estimating the effects of potential climate and land use changes on hydrologic processes of a large agriculture dominated watershed. J. Hydrol. 529, 418–429.
Nie, W., Yuan, Y., Kepner, W., Nash, M., Jackson, M., Erickson, C., 2011. Assessing impacts of land use and land cover changes on hydrology for the upper San Pedro watershed. J. Hydrol. 407, 105–114.
Omar, N., Ahamad, M., Hussin, W., Samat, N., Ahmad, S., 2014. Markov CA, multi regression, and multiple decision making for modeling historical changes in Kirkuk City, Iraq. J. Indian Soc. Remote Sens. 42 (1), 165–178.
Pontius, R., Schneider, L., 2001. Land-cover change model validation by an ROC method for the Ipswich watershed, Massachusetts, USA. Agric. Ecosyst. Environ. 85, 239–248.
Rientjes, T., Haile, A., Kebede, E., Mannaerts, C., Habib, E., Steenhuis, T., 2011. Changes in land cover, rainfall and streamflow in Upper Gilgel Abbay catchment, Blue Nile basin — Ethiopia. Hydrol. Earth Syst. Sci. 15, 1979–1989.
SAS Institute Inc., 2017. JMP® 13 Multivariate Methods. Second edition. SAS Institute Inc., Cary, NC 230 pp.
Setegn, S., Srinivasan, R., Dargahi, B., 2008. Hydrological modelling in the Lake Tana basin, Ethiopia using SWAT model. Open Hydrol. J. 2, 49–62.
Setegn, S., Srinivasan, R., Dargahi, B., Melesse, A., 2009. Spatial delineation of soil erosion vulnerability in the Lake Tana Basin, Ethiopia. Hydrol. Process. https://doi.org/10.1002/hyp.7476.
Shapiro, S., Wilk, M., 1965. An analysis of variance test for normality (complete samples). Biometrika 52 (3–4), 591–611.
Shi, Z., Ai, L., Li, X., Huang, X., Wu, G., Liao, W., 2013. Partial least-squares regression for linking land-cover patterns to soil erosion and sediment yield in watersheds. J. Hydrol. 498, 165–176.
Singh, S., Mustak, S., Srivastava, P., Szabó, S., Islam, T., 2015. Predicting spatial and decadal LULC changes through Cellular Automata Markov Chain models using earth observation datasets and geo-information. Environ. Process. 2, 61–78.
Siriwardena, L., Finlayson, B., McMahon, T., 2006. The impact of land use change on catchment hydrology in large catchments: the Comet River, Central Queensland, Australia. J. Hydrol. 326, 199–214.
Solomon, G., Ayele, T., Bishop, K., 2010. Forest cover and streamflow in a headwater of the Blue Nile: complementing observational data analysis with community perception. Ambio 39 (4), 284–294.
Solomon, G., Woldeamlak, B., Gärdenäs, A., Bishop, K., 2014. Forest cover change over four decades in the Blue Nile Basin, Ethiopia: comparison of three watersheds. Reg. Environ. Change 14, 253–266.
Sriwongsitanon, N., Taesombat, W., 2011. Effects of land cover on runoff coefficient. J. Hydrol. 410, 226–238.
Tang, F., Xu, H., Xu, Z., 2012. Model calibration and uncertainty analysis for runoff in the Chao River Basin using sequential uncertainty fitting. Procedia Environ. Sci. 13, 1760–1770.
Teferi, E., Uhlenbrook, S., Bewket, W., Wenninger, J., Simane, B., 2010. The use of remote sensing to quantify wetland loss in the Choke Mountain range, Upper Blue Nile basin, Ethiopia. Hydrol. Earth Syst. Sci. 14, 2415–2428.
Tekalegn, A., Elagib, N., Ribbe, L., Heinrich, J., 2017. Hydrological responses to land use/cover changes in the source region of the Upper Blue Nile Basin, Ethiopia. Sci. Total Environ. 575, 724–741.
Tekleab, S., Mohamed, Y., Uhlenbrook, S., 2013. Hydro-climatic trends in the Abay/upper Blue Nile basin, Ethiopia. Phys. Chem. Earth 61-62, 32–42.
Temesgen, G., Amare, B., Abraham, M., 2014. Evaluations of land use/land cover changes and land degradation in Dera District, Ethiopia: GIS and remote sensing based analysis. Int. J. Sci. Res. Environ. Sci. 2 (6), 199–208.
Temesgen, G., Taffa, T., Mekuria, A., Abeyou, W., 2017. Evaluation and prediction of land use/land cover changes in the Andassa watershed, Blue Nile Basin, Ethiopia. Environ. Syst. Res. 6 (17), 1–15.
Tibebe, D., Bewket, W., 2011. Surface runoff and soil erosion estimation using the SWAT model in the Keleta watershed, Ethiopia. Land Degrad. Dev. 22, 551–564.
Uhlenbrook, S., Mohamed, Y., Gragne, A., 2010. Analyzing catchment behavior through catchment modeling in the Gilgel Abay, Upper Blue Nile River Basin, Ethiopia. Hydrol. Earth Syst. Sci. 14, 2153–2165.
USDA-SCS (United States Department of Agriculture–Soil Conservation Service), 1972. National Engineering Handbook, Section 4 Hydrology. USDA, Washington, DC.
Vilaysane, B., Takara, K., Luo, P., Akkharath, I., Duan, W., 2015. Hydrological streamflow modelling for calibration and uncertainty analysis using SWAT model in the Xedone river basin, Lao PDR. Procedia Environ. Sci. 28, 380–390.
Wang, S., Zheng, X., Zang, X., 2012. Accuracy assessments of land use change simulation based on Markov-Cellular Automata model. Procedia Environ. Sci. 13, 1238–1245.
Wold, S., Sjöström, M., Eriksson, L., 2001. PLS-regression: a basic tool of chemometrics. Chemom. Intell. Lab. Syst. 58 (2), 109–130.
Woldeamlak, B., 2002. Land cover dynamics since the 1950s in Chemoga watershed, Blue Nile basin, Ethiopia. Mt. Res. Dev. 22 (3), 263–269.
Woldeamlak, B., Sterk, G., 2005. Dynamics in land cover and its effect on streamflow in the Chemoga watershed, Blue Nile basin, Ethiopia. Hydrol. Process. 19, 445–458.
Yan, B., Fang, N., Zhang, P., Shi, Z., 2013. Impacts of land use change on watershed streamflow and sediment yield: an assessment using hydrologic modeling and partial least squares regression. J. Hydrol. 484, 26–37.
Zhou, J., Liu, Y., Guo, H., He, D., 2014. Combining the SWAT model with sequential uncertainty fitting algorithm for streamflow prediction and uncertainty analysis for the Lake Dianchi Basin, China. Hydrol. Process. 28, 521–533.